Results on Proton-Induced Reactions of ^{238}U

Gabriel García Jiménez

R^{3}B Collaboration Meeting 2024, GSI.

Proposed Experiment

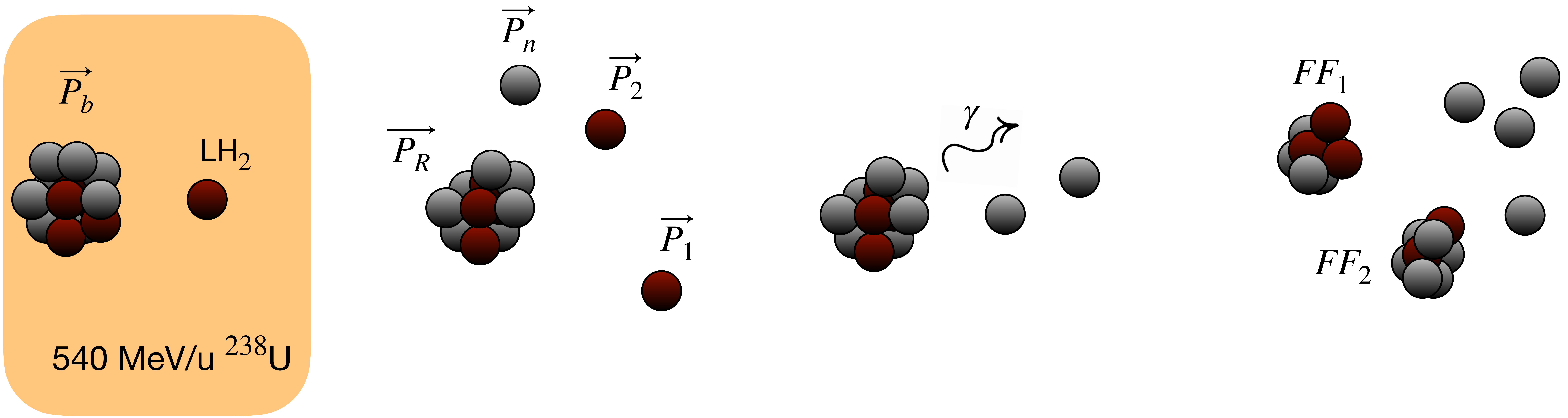

$$\begin{pmatrix} E_b \\ 0 \\ 0 \\ p_{bz} \end{pmatrix} + \begin{pmatrix} m_t c^2 \\ 0 \\ 0 \\ 0 \end{pmatrix} = \begin{pmatrix} E_1 \\ p_{1x}c \\ p_{1y}c \\ p_{1z}c \end{pmatrix} + \begin{pmatrix} E_2 \\ p_{2x}c \\ p_{2y}c \\ p_{2z}c \end{pmatrix} + \begin{pmatrix} E_R \\ p_{Rx}c \\ p_{Ry}c \\ p_{Rz}c \end{pmatrix} \Rightarrow I_m^2 = \left(\sum E\right)^2 - \left|\sum pc\right|^2 \rightarrow \boxed{E^* = I_m - m_R c^2}$$

Proposed Experiment

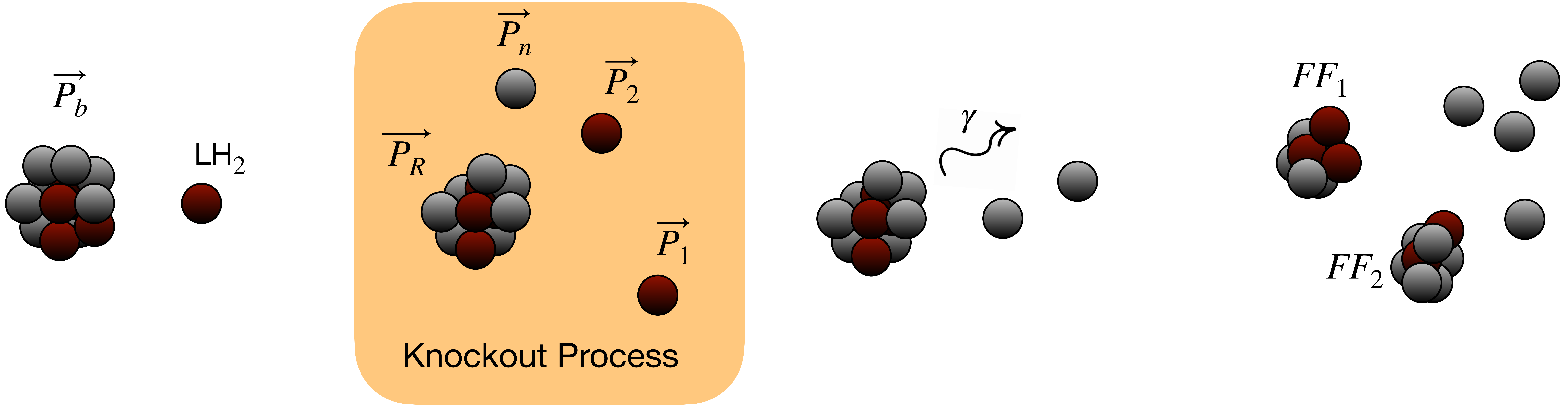

$$\begin{pmatrix} E_b \\ 0 \\ 0 \\ p_{bz} \end{pmatrix} + \begin{pmatrix} m_t c^2 \\ 0 \\ 0 \\ 0 \end{pmatrix} = \begin{pmatrix} E_1 \\ p_{1x}c \\ p_{1y}c \\ p_{1z}c \end{pmatrix} + \begin{pmatrix} E_2 \\ p_{2x}c \\ p_{2y}c \\ p_{2z}c \end{pmatrix} + \begin{pmatrix} E_R \\ p_{Rx}c \\ p_{Ry}c \\ p_{Rz}c \end{pmatrix} \Rightarrow I_m^2 = \left(\sum E\right)^2 - \left|\sum pc\right|^2 \rightarrow \boxed{E^* = I_m - m_R c^2}$$

Proposed Experiment

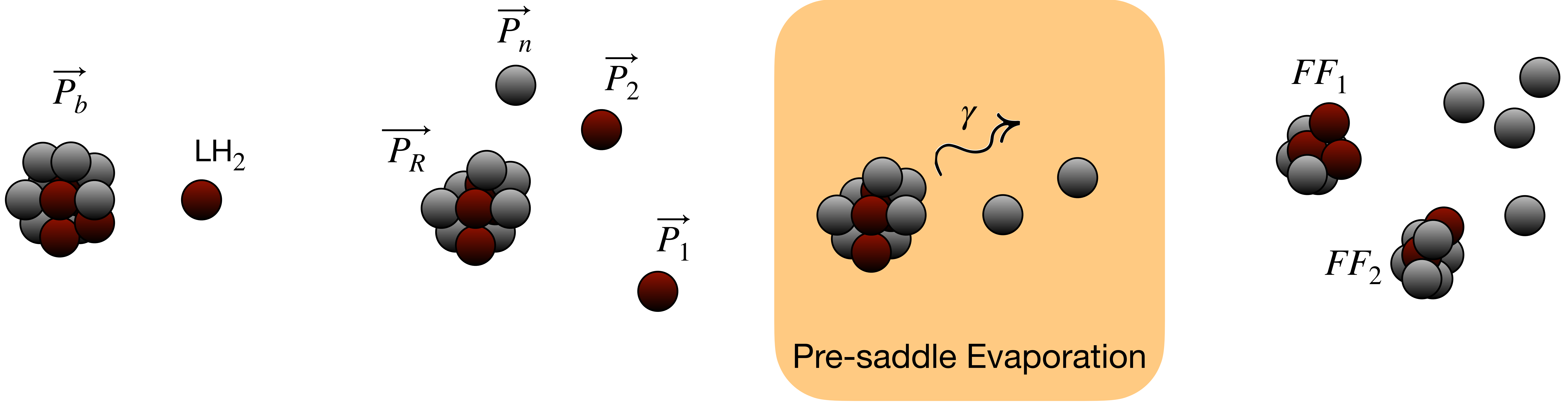

$$\begin{pmatrix} E_b \\ 0 \\ 0 \\ p_{bz} \end{pmatrix} + \begin{pmatrix} m_t c^2 \\ 0 \\ 0 \\ 0 \end{pmatrix} = \begin{pmatrix} E_1 \\ p_{1x}c \\ p_{1y}c \\ p_{1z}c \end{pmatrix} + \begin{pmatrix} E_2 \\ p_{2x}c \\ p_{2y}c \\ p_{2z}c \end{pmatrix} + \begin{pmatrix} E_R \\ p_{Rx}c \\ p_{Ry}c \\ p_{Rz}c \end{pmatrix} \Rightarrow I_m^2 = \left(\sum E\right)^2 - \left|\sum pc\right|^2 \rightarrow \boxed{E^* = I_m - m_R c^2}$$

Proposed Experiment

$$\begin{pmatrix} E_b \\ 0 \\ 0 \\ p_{bz} \end{pmatrix} + \begin{pmatrix} m_t c^2 \\ 0 \\ 0 \\ 0 \end{pmatrix} = \begin{pmatrix} E_1 \\ p_{1x}c \\ p_{1y}c \\ p_{1z}c \end{pmatrix} + \begin{pmatrix} E_2 \\ p_{2x}c \\ p_{2y}c \\ p_{2z}c \end{pmatrix} + \begin{pmatrix} E_R \\ p_{Rx}c \\ p_{Ry}c \\ p_{Rz}c \end{pmatrix} \Rightarrow I_m^2 = \left(\sum E\right)^2 - \left|\sum pc\right|^2 \rightarrow \boxed{E^* = I_m - m_R c^2}$$

Motivations: Damping of the Shell Effects

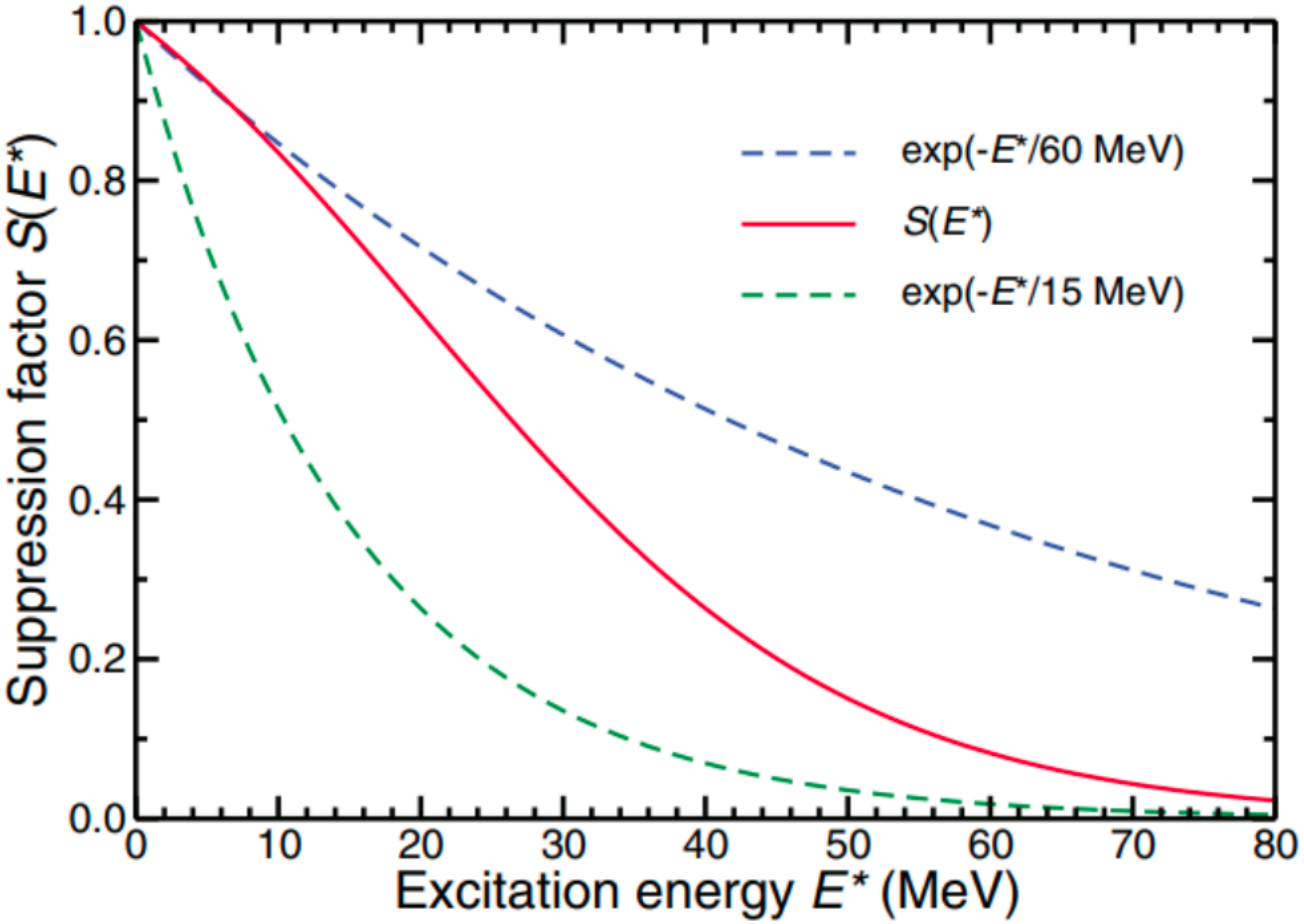

J. Randrup and P. Moller. Energy dependence of fission-fragment mass distributions from strongly damped shape evolution. Physical Review C, 2013.

$$E = E_{LDM} + S(E^*)\ \delta E_{Shell} + E_{Pairing}$$

Different Functions Proposed:

$$S(E^*) = \exp(-E^*/E_0)$$ (A. V. Ignatyuk)

$$S(E^*) = \frac{1 + e^{-E_1/E_0}}{1 + e^{(E^* - E_1)/E_0}}$$ (J. Randrup, P. Möller)

$$S(E^*) = \exp(-E^*/\rho(E^*))$$ (ABLA07)

Motivations: Superfluid Phase

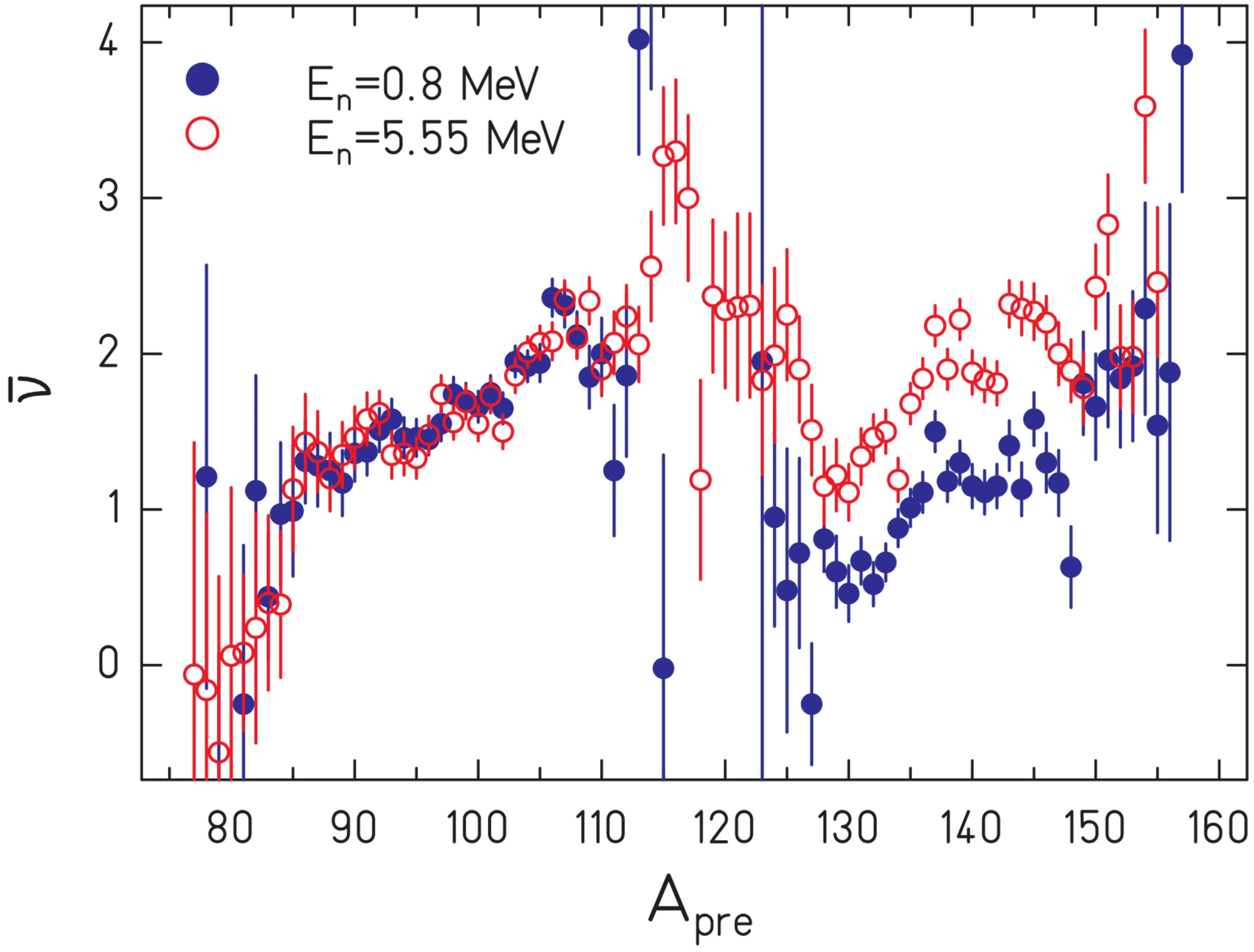

Superfluid Behaviour: Energy Sorting Mechanism

- Neutron evaporation increases only for the heavy fragment, when more E* is added to the system.
- Particle flow from the light to the heavy fragment. $\Delta S > 0$.
- E* < 20 MeV, for medium-mass isotopes.

Karl-Heinz Schmidt and Beatriz Jurado, Entropy Driven Excitation Energy Sorting in Superfluid Fission Dynamics. PRL. 2010.

The R3B/SOFIA Experimental Setup

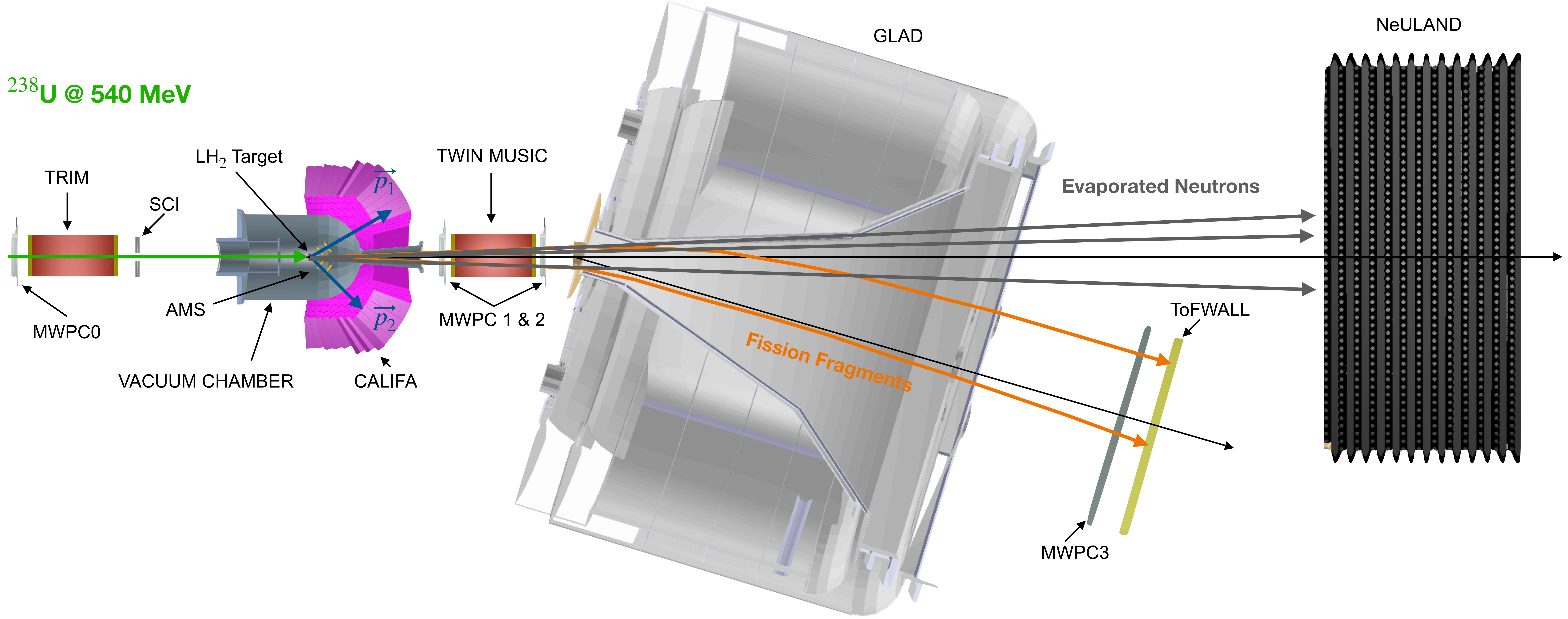

Data Analysis

Data Analysis Overview

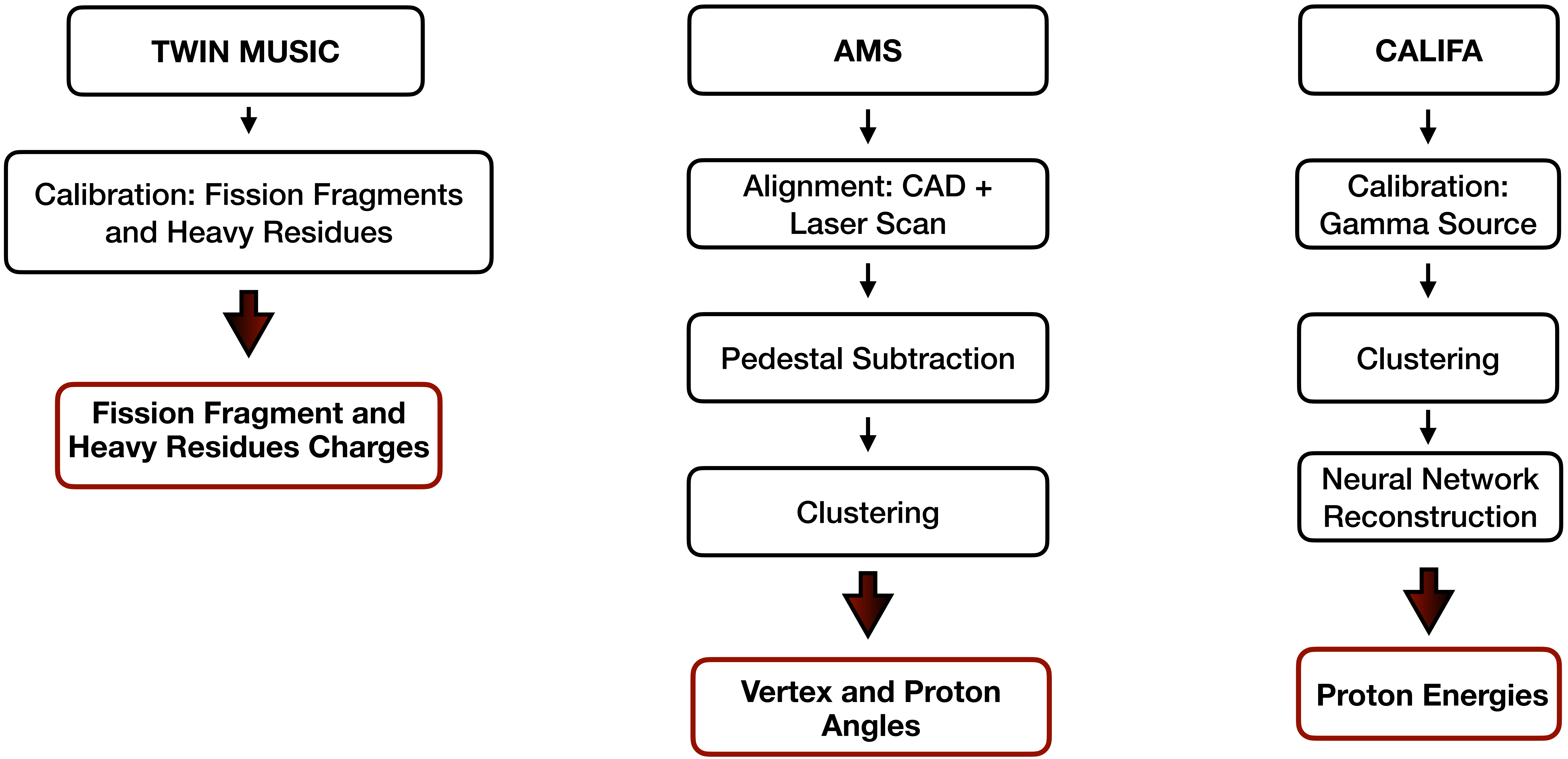

Data Analysis Overview

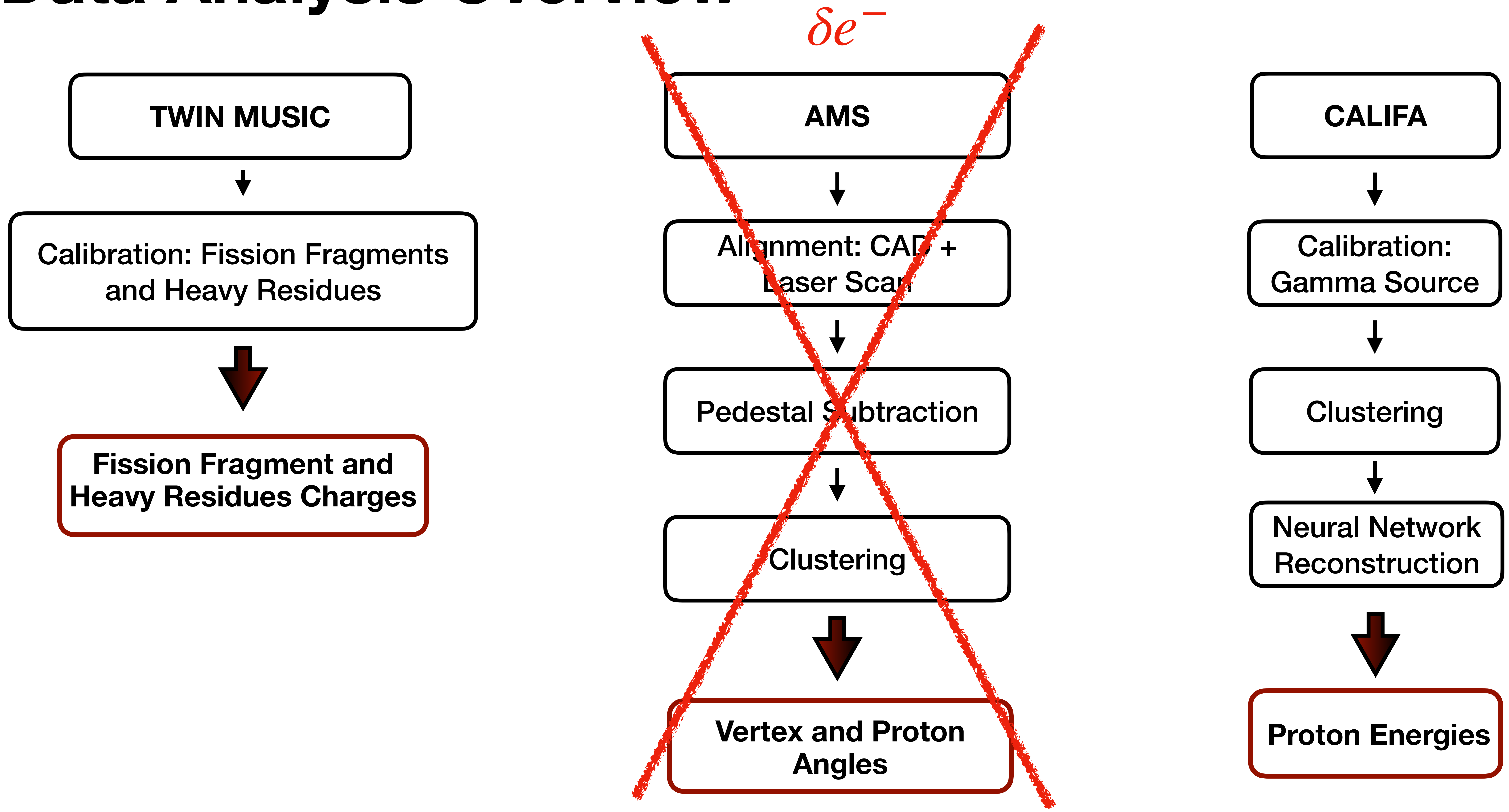

Data Analysis Overview

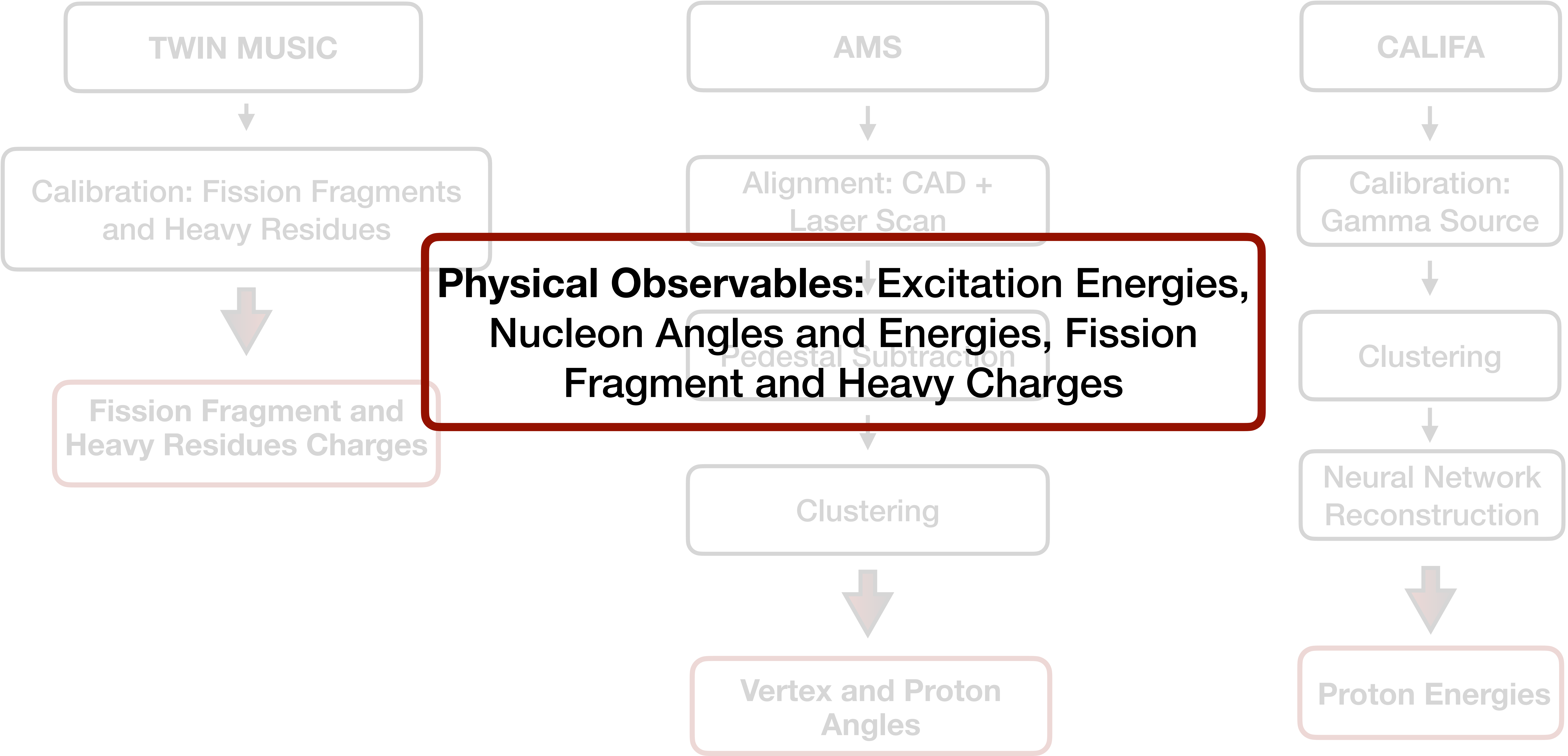

Results and Discussion

Fissioning Systems

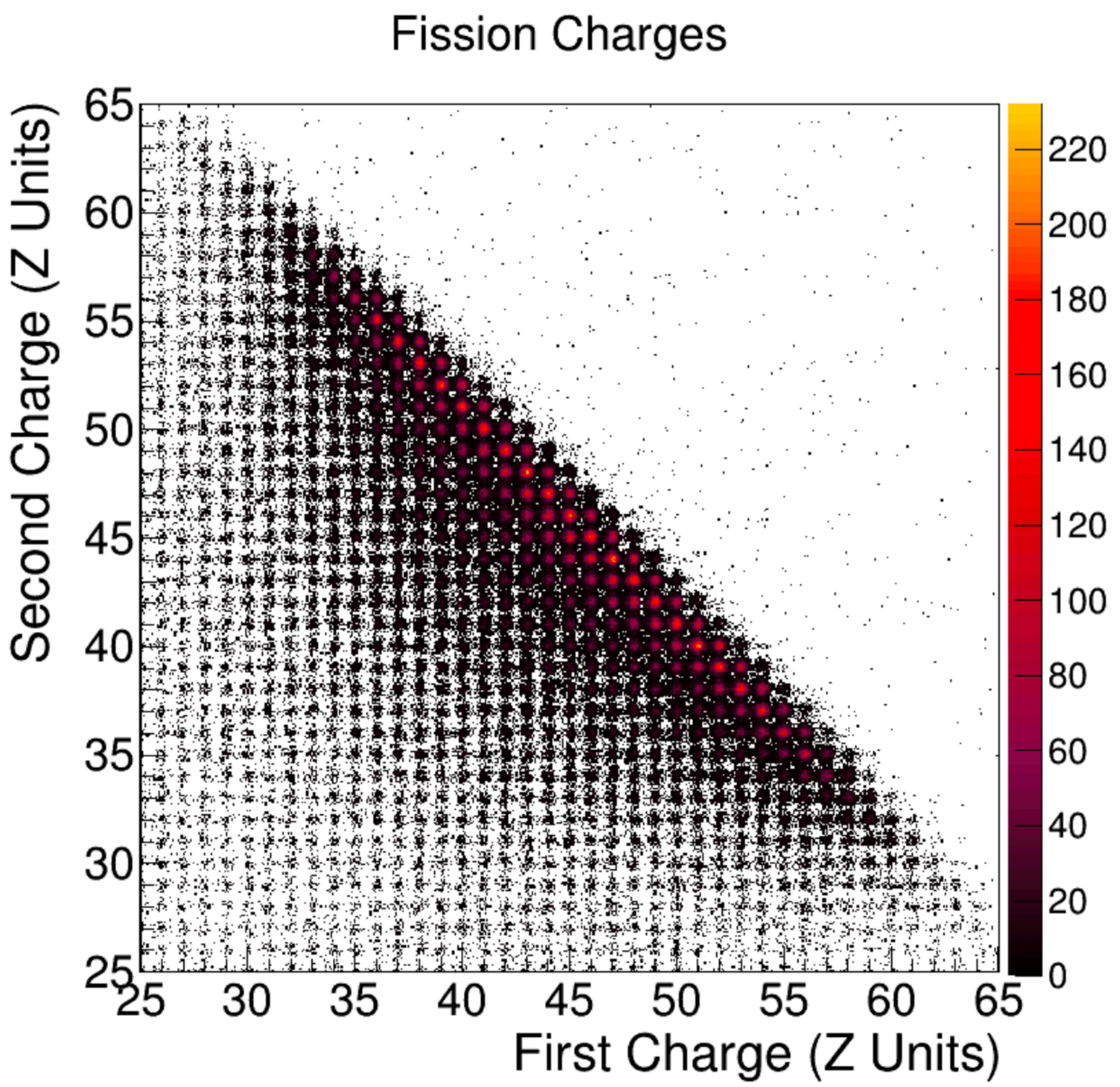

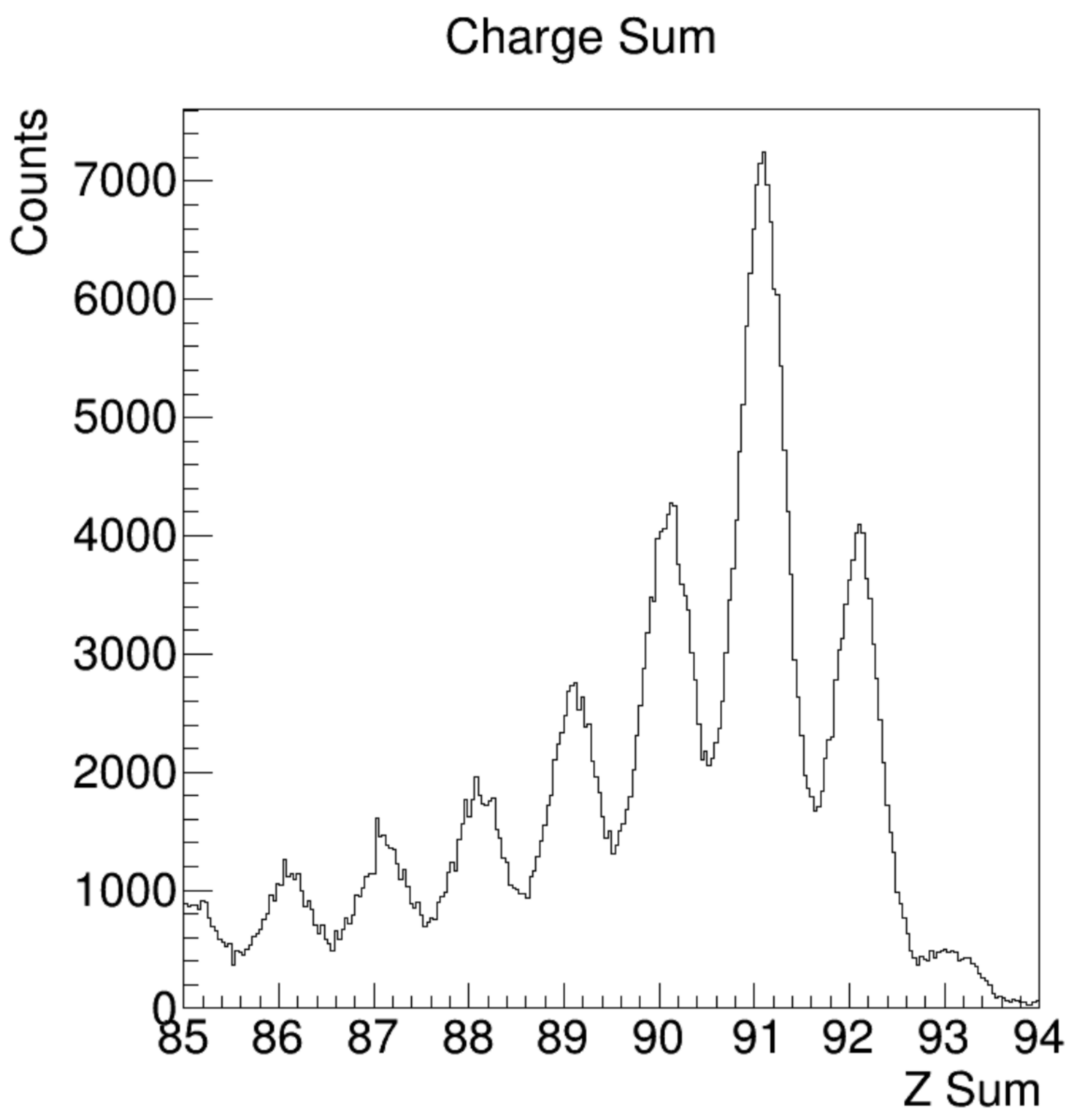

Fissioning Systems

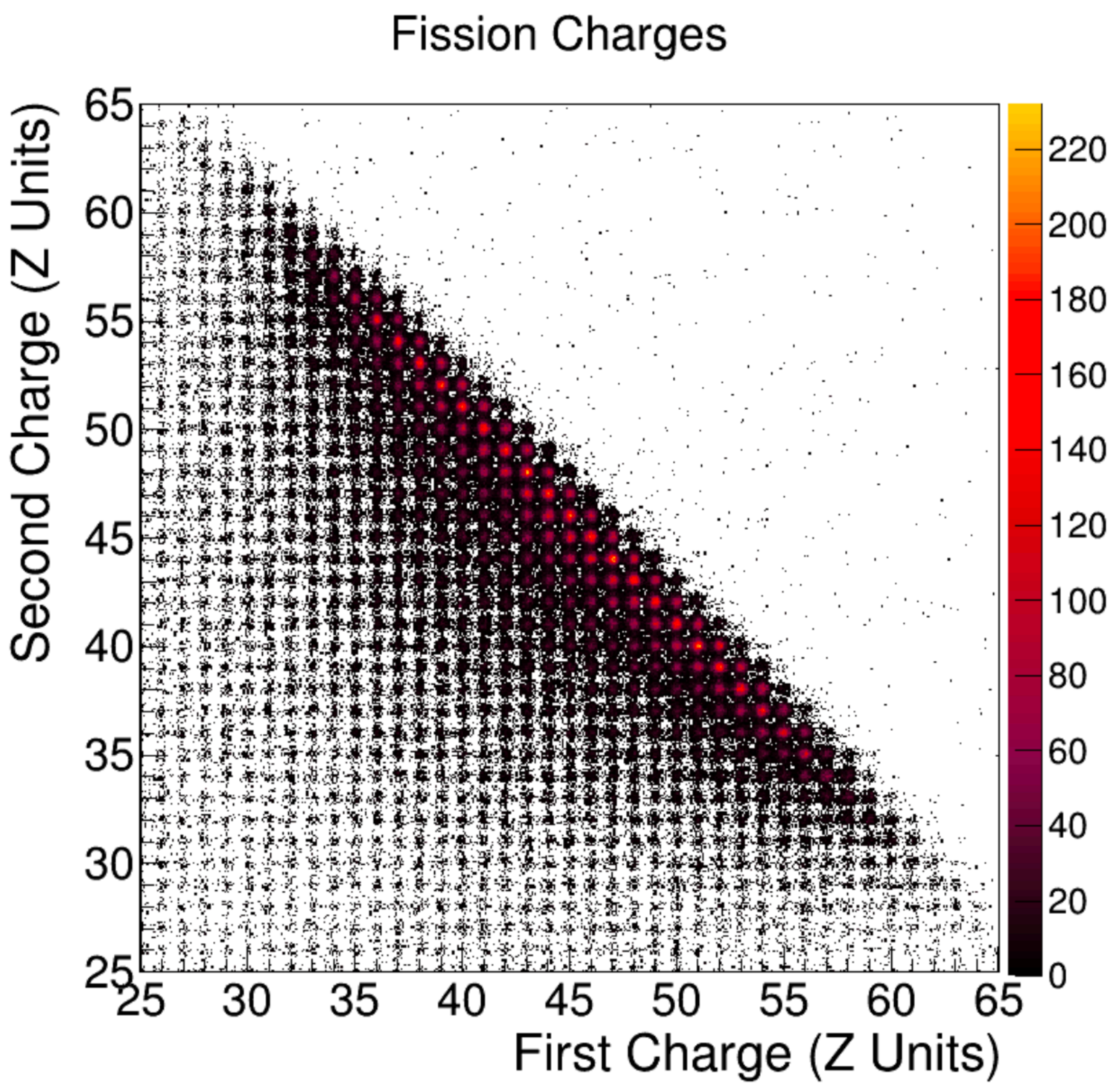

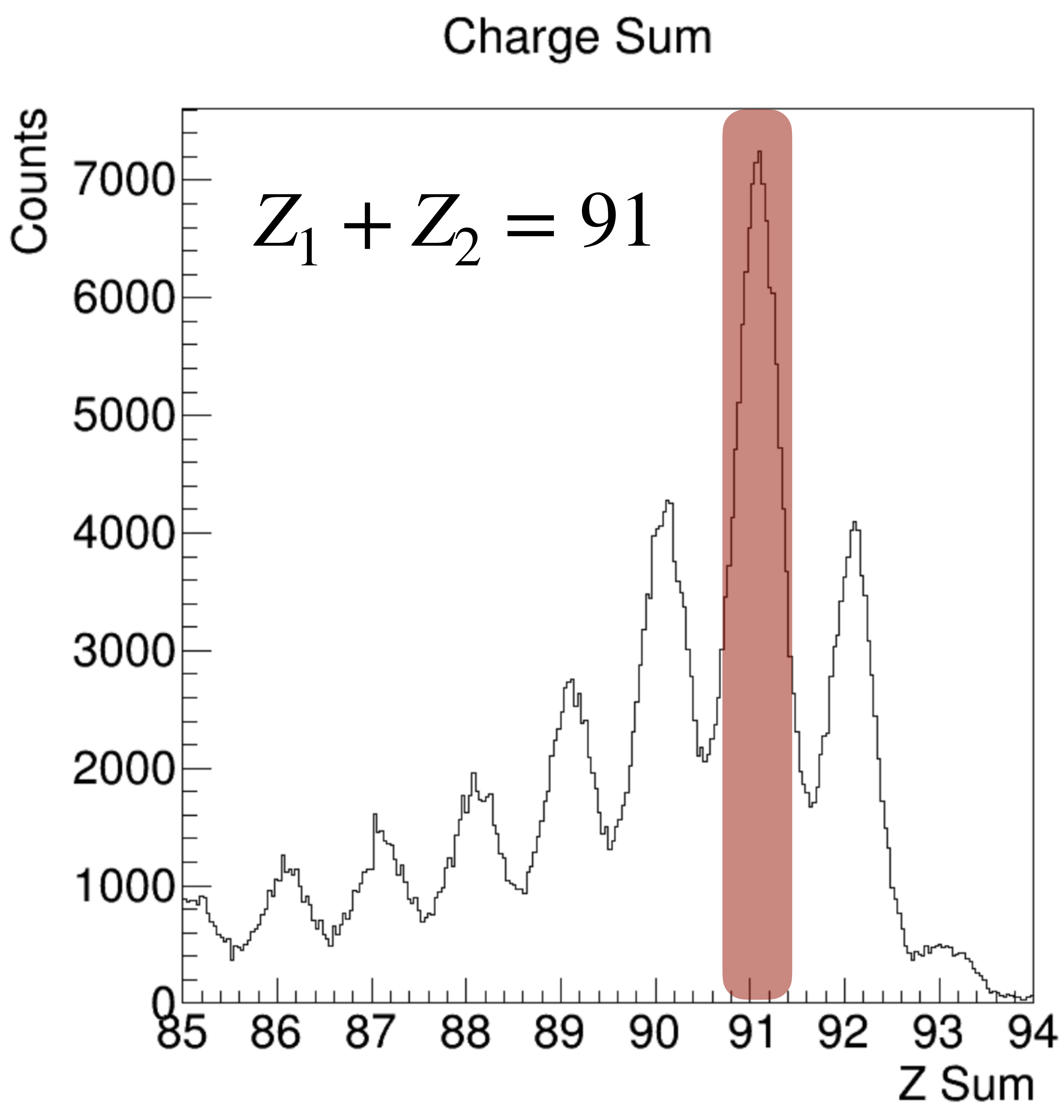

Theoretical Fissioning Systems

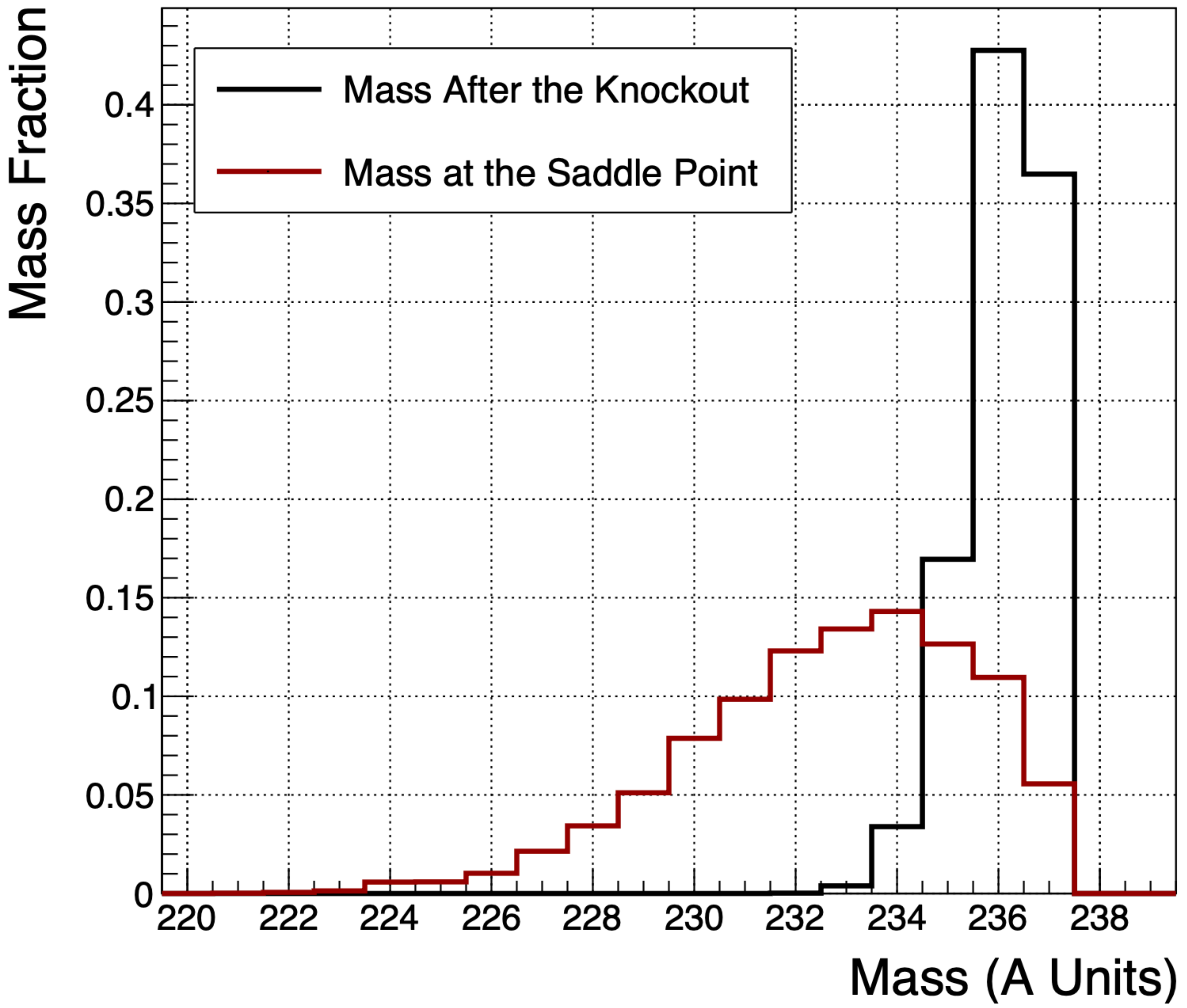

- INCL simulations show different knockout reaction channels before fission: (p,2p), (p,2pn), (p,2p2n)…
- The excitation energy calculation is only valid for the two-proton removal channel.
- For the rest the missing energy is shared between excitation energy and kinetic energy of the non-measured neutrons.
- Neutron evaporation at the pre-saddle stage is also expected, resulting in different fissioning systems.

Opening Angle Distributions

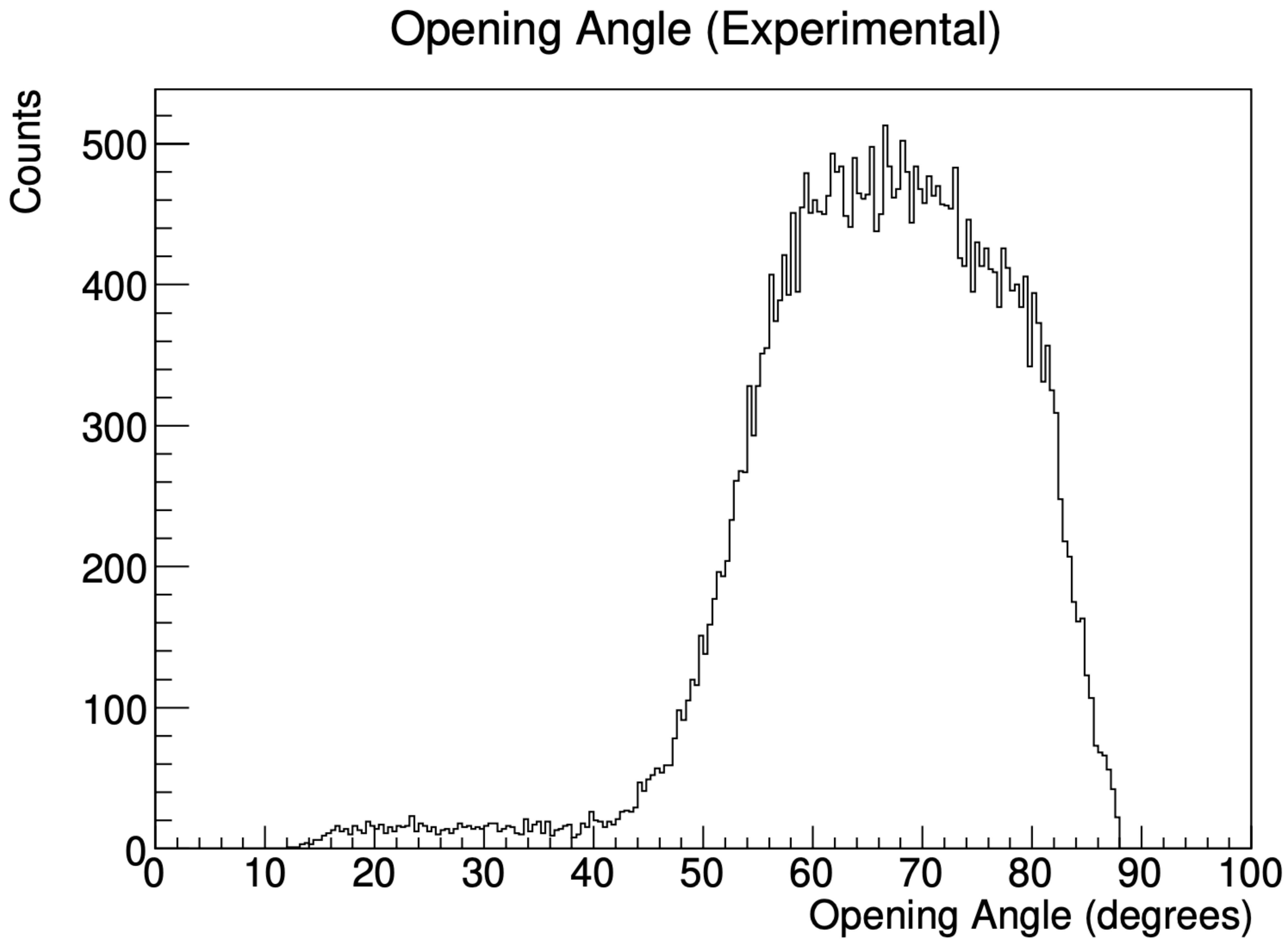

$$\alpha = \cos^{-1}\left[\sin(\theta_1)\sin(\theta_2)\cos(\phi_2 - \phi_1) + \cos(\theta_1)\cos(\theta_2)\right]$$

Different contributions:

- Quasi-free knockout
- Re-scattering processes
- Multi-nucleon knockout

Opening Angle Distributions

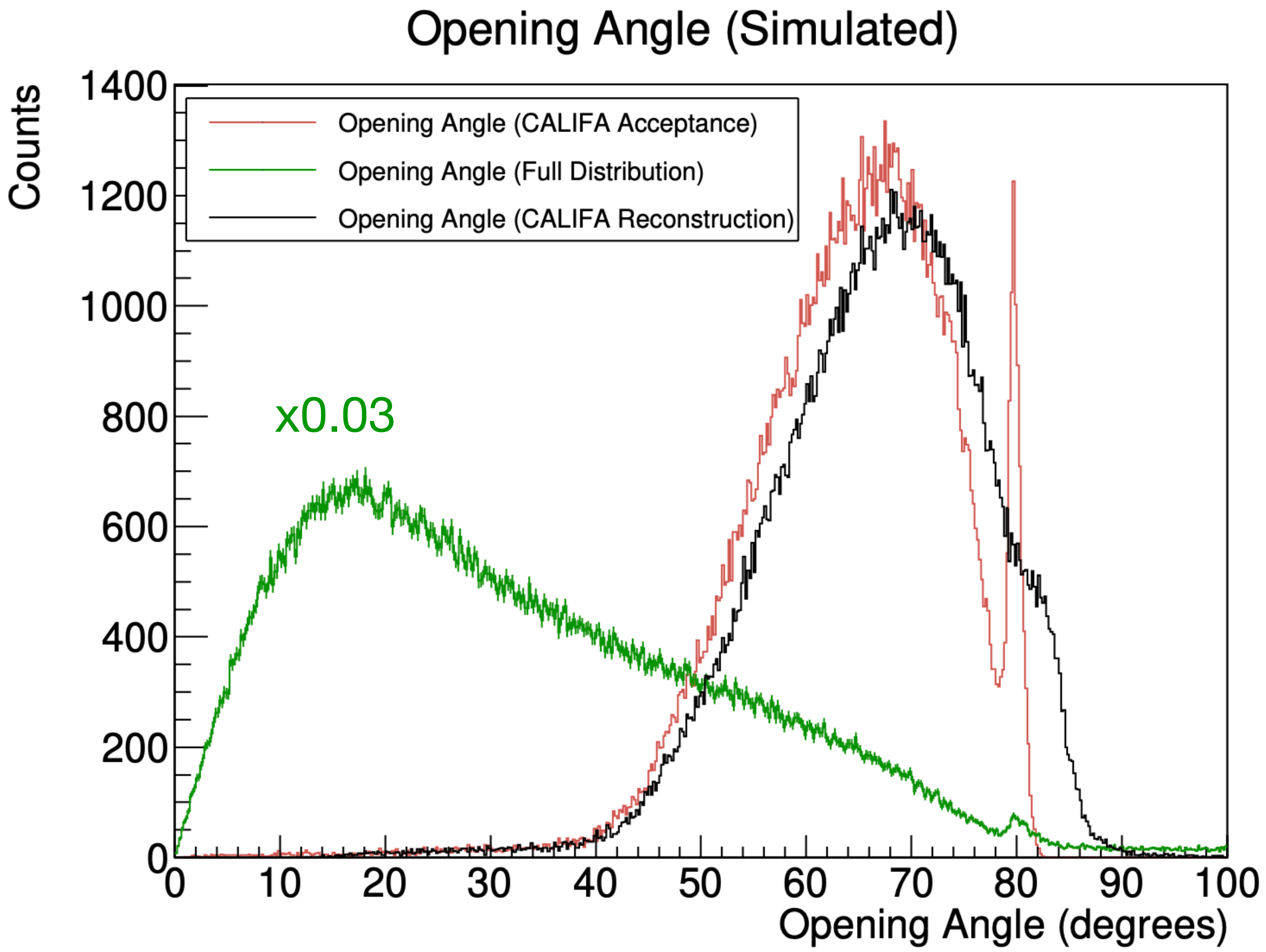

$$\hat{\alpha} = \cos^{-1}\left[\sin(\theta_1)\sin(\theta_2)\cos(\phi_2 - \phi_1) + \cos(\theta_1)\cos(\theta_2)\right]$$

Different contributions:

- Quasi-free knockout
- Re-scattering processes
- Multi-nucleon knockout

Kinematic Distributions

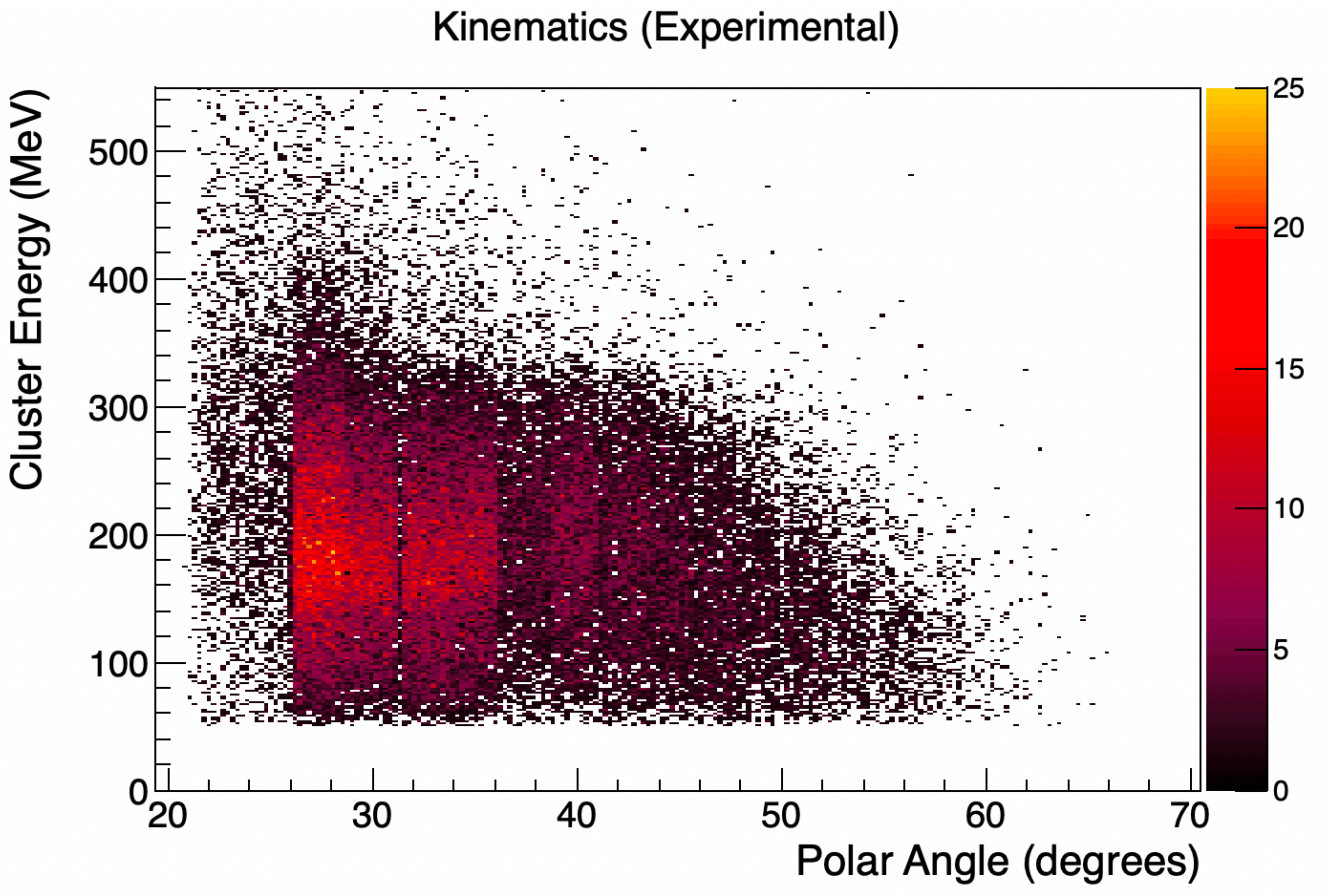

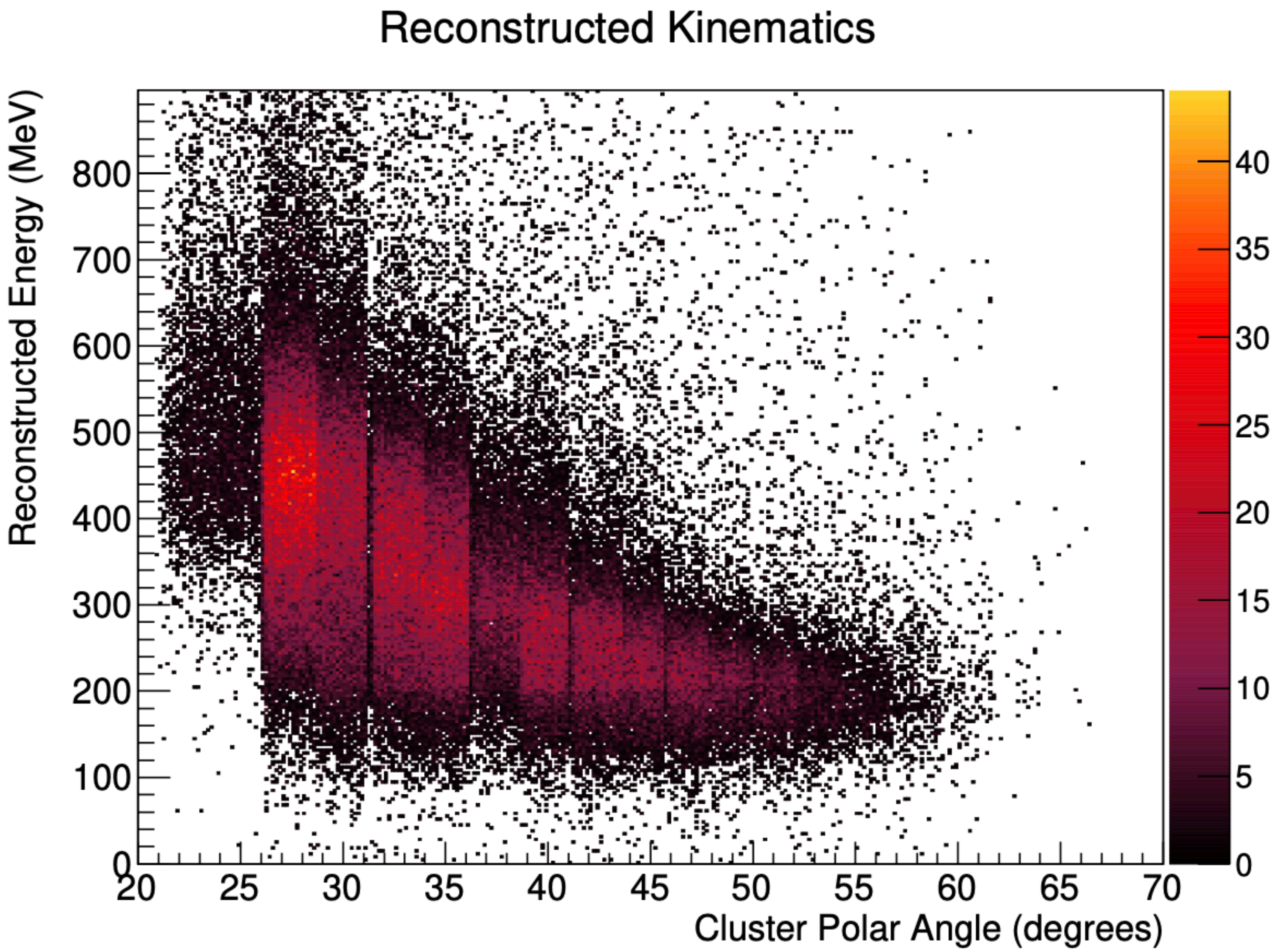

Missing Energy

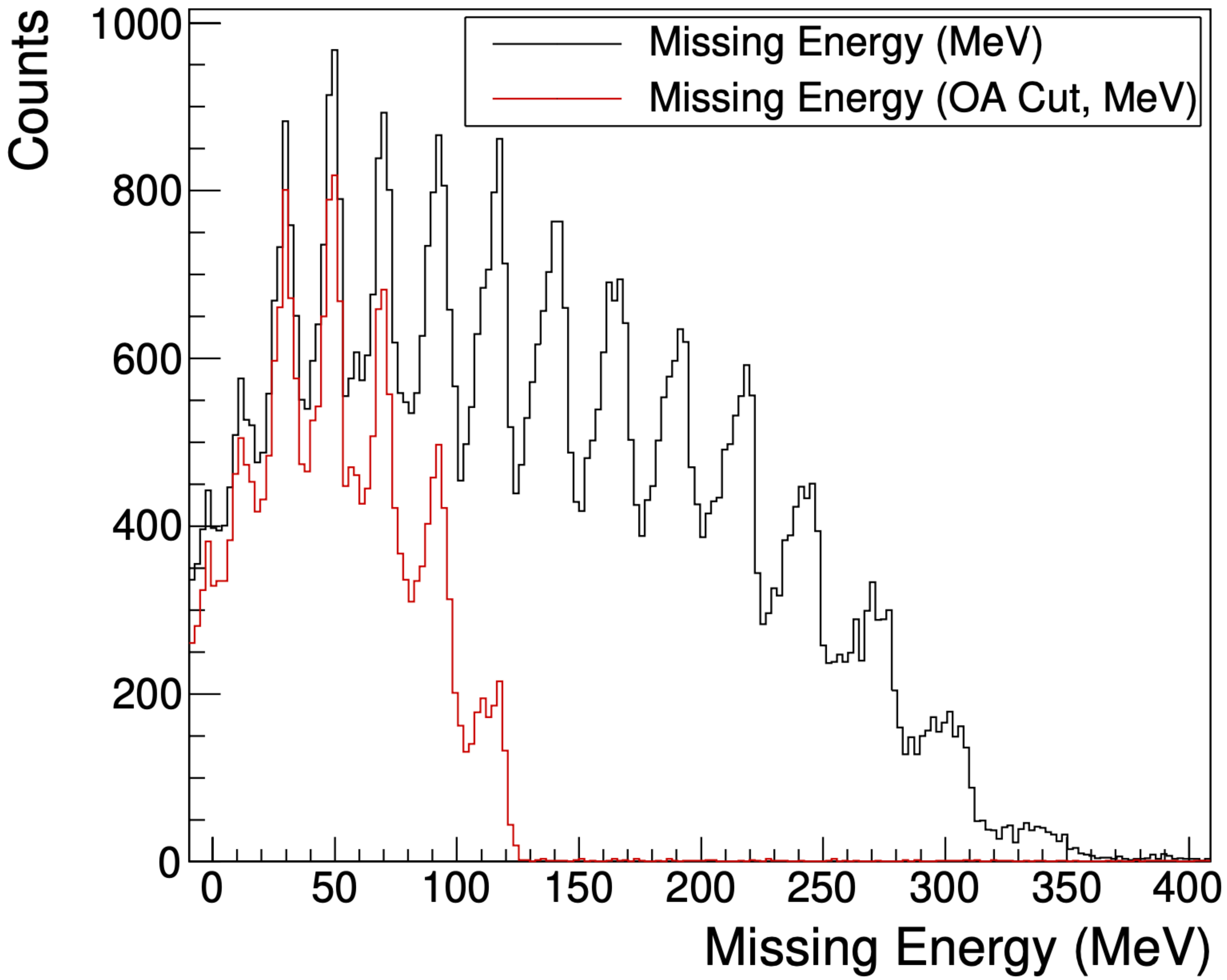

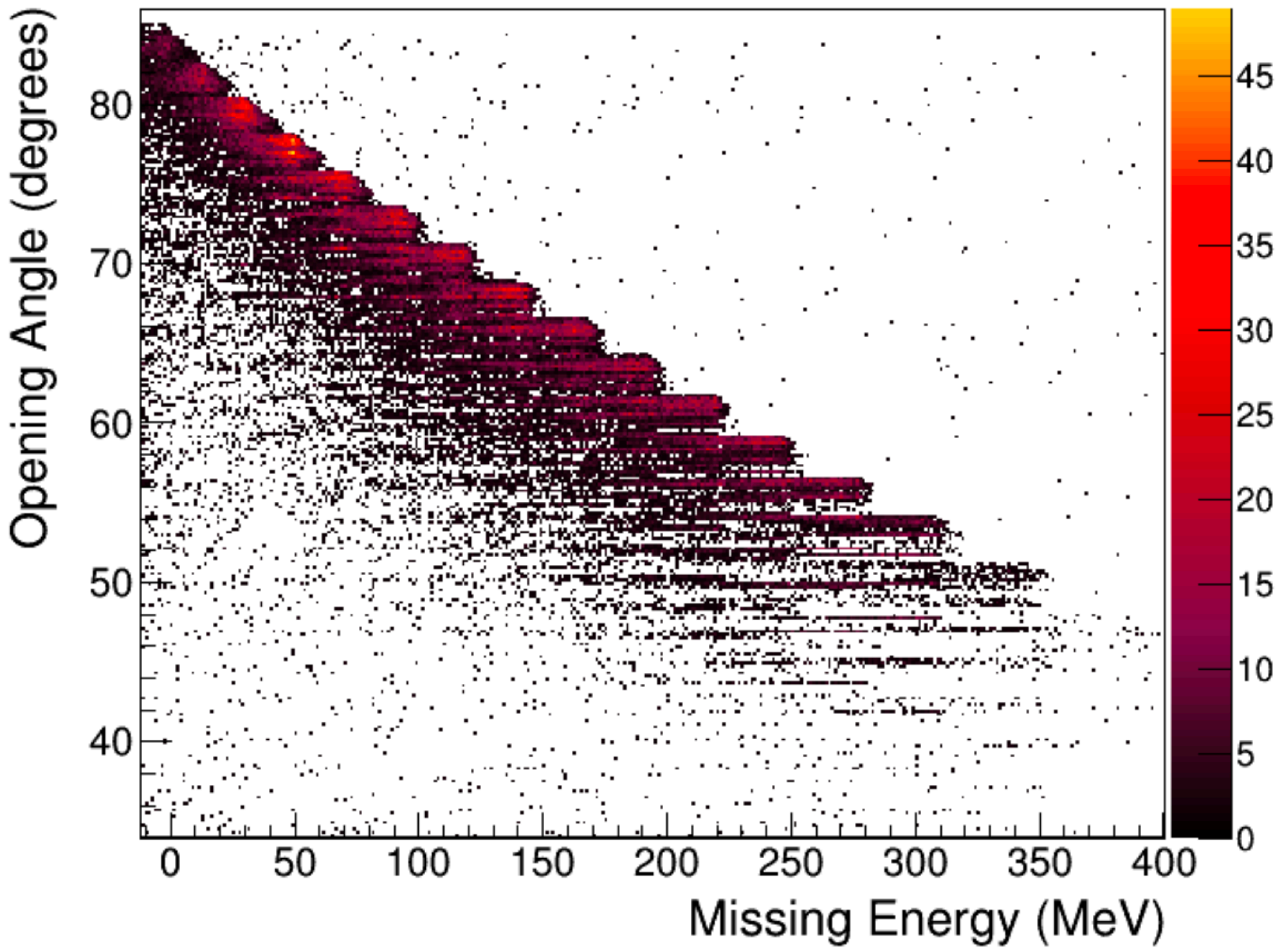

Fission Fragment Evolution: Opening Angle

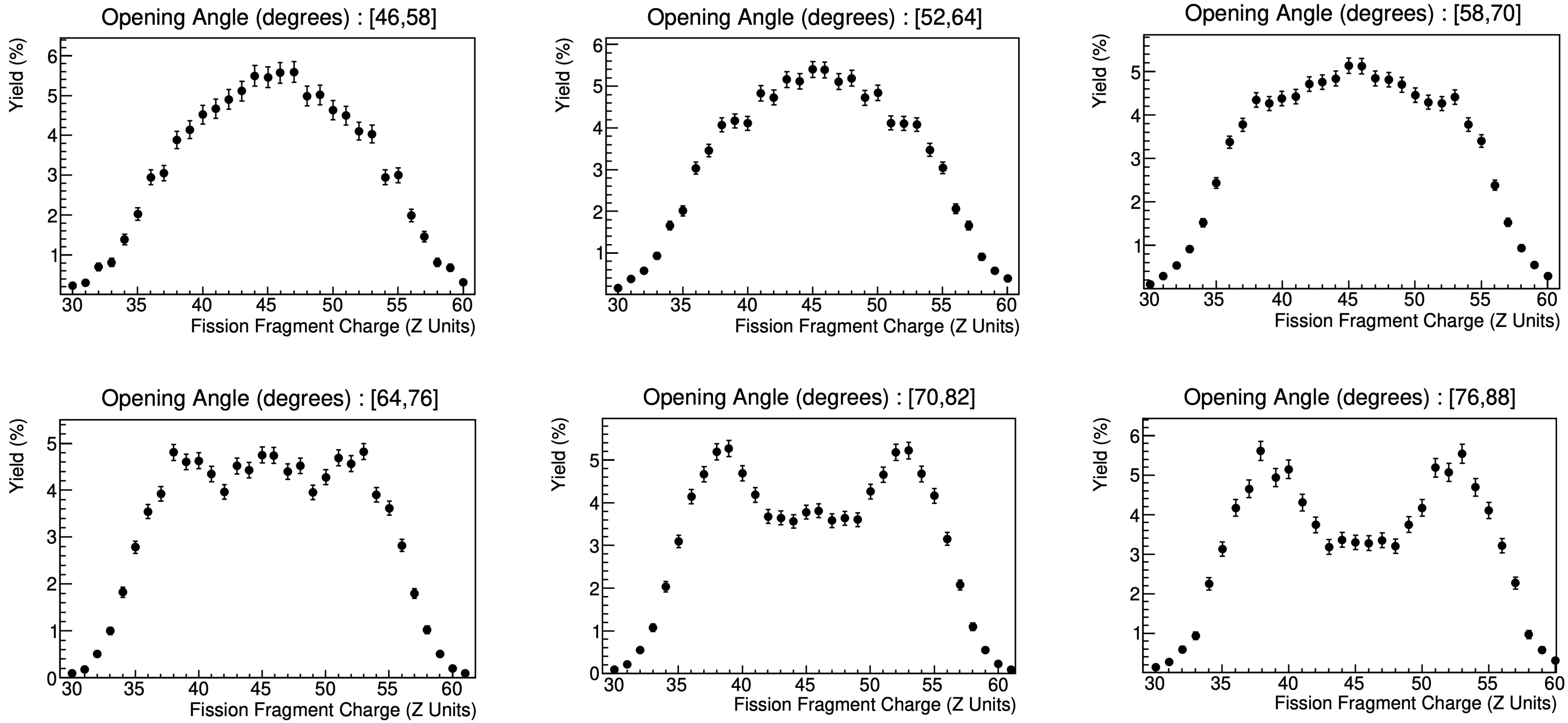

Charge yields defined as: $Y(Z) = \sum_{A} Y(Z, A)$

Fission Fragment Evolution: Missing Energy

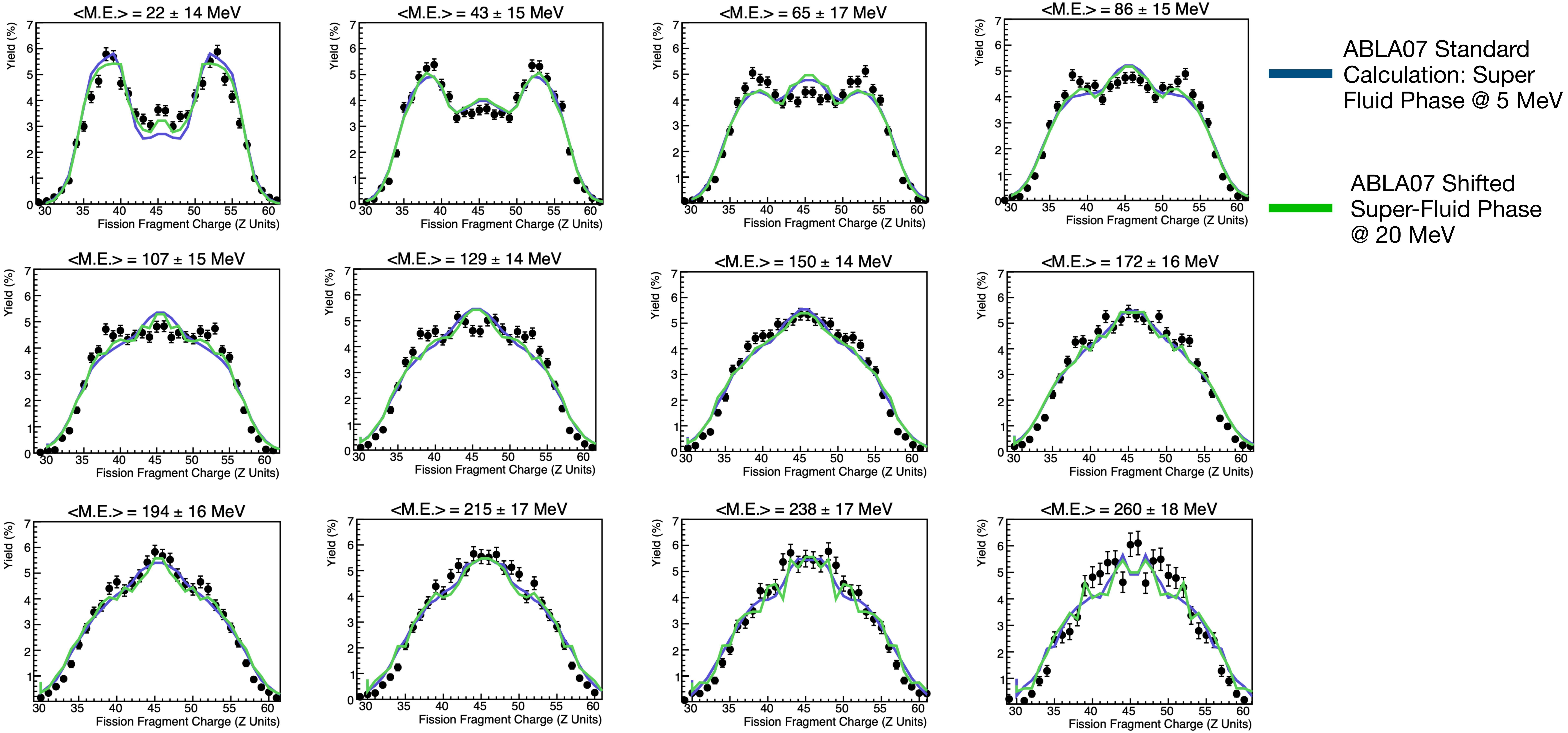

Fission Fragment Evolution: Missing Energy

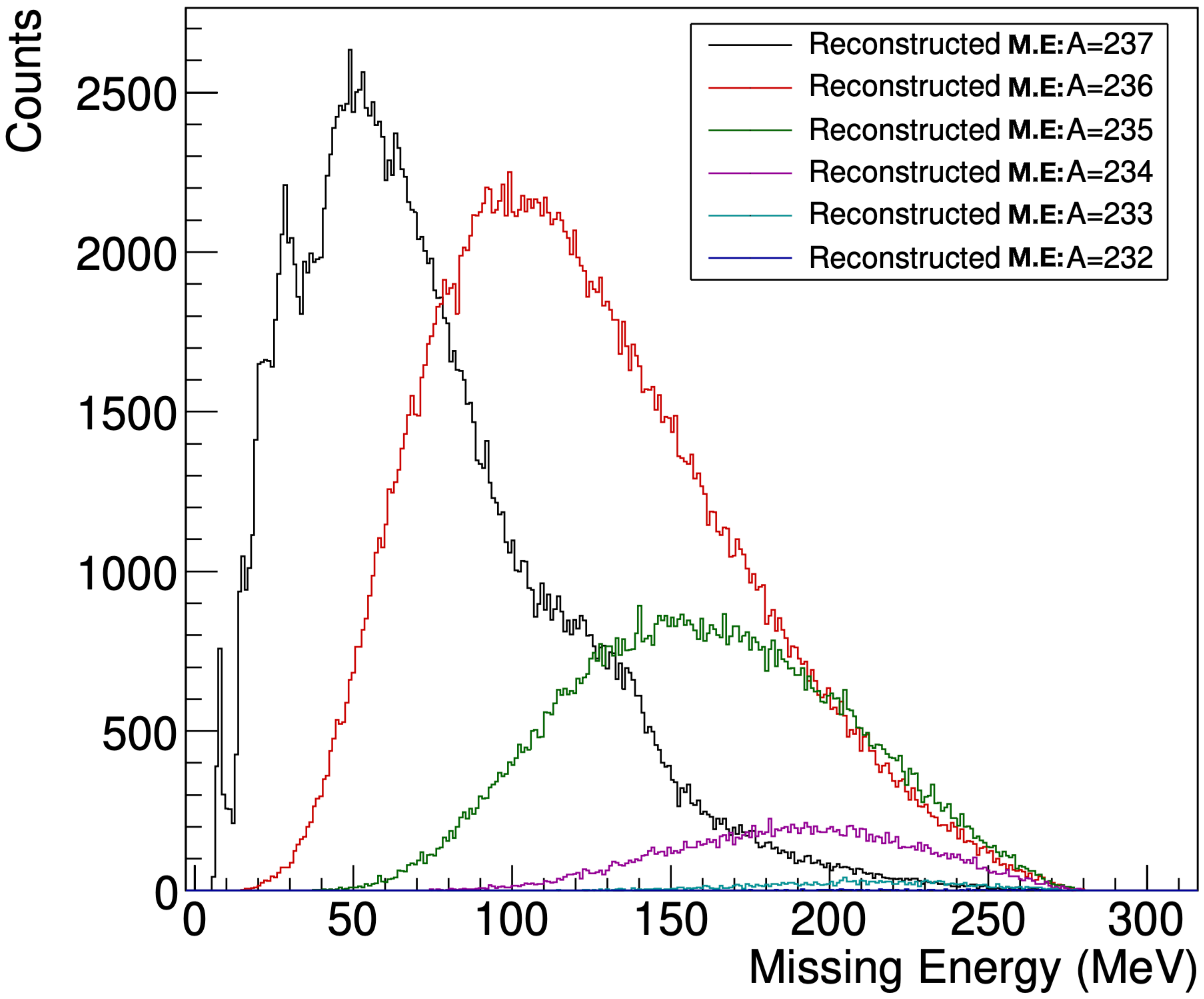

- Different isotopes at the end of the intra-nuclear cascade.
- The two-proton calculation yields displaced missing energy distributions.
- They can not be disentangled.

Fission Fragment Evolution: Missing Energy

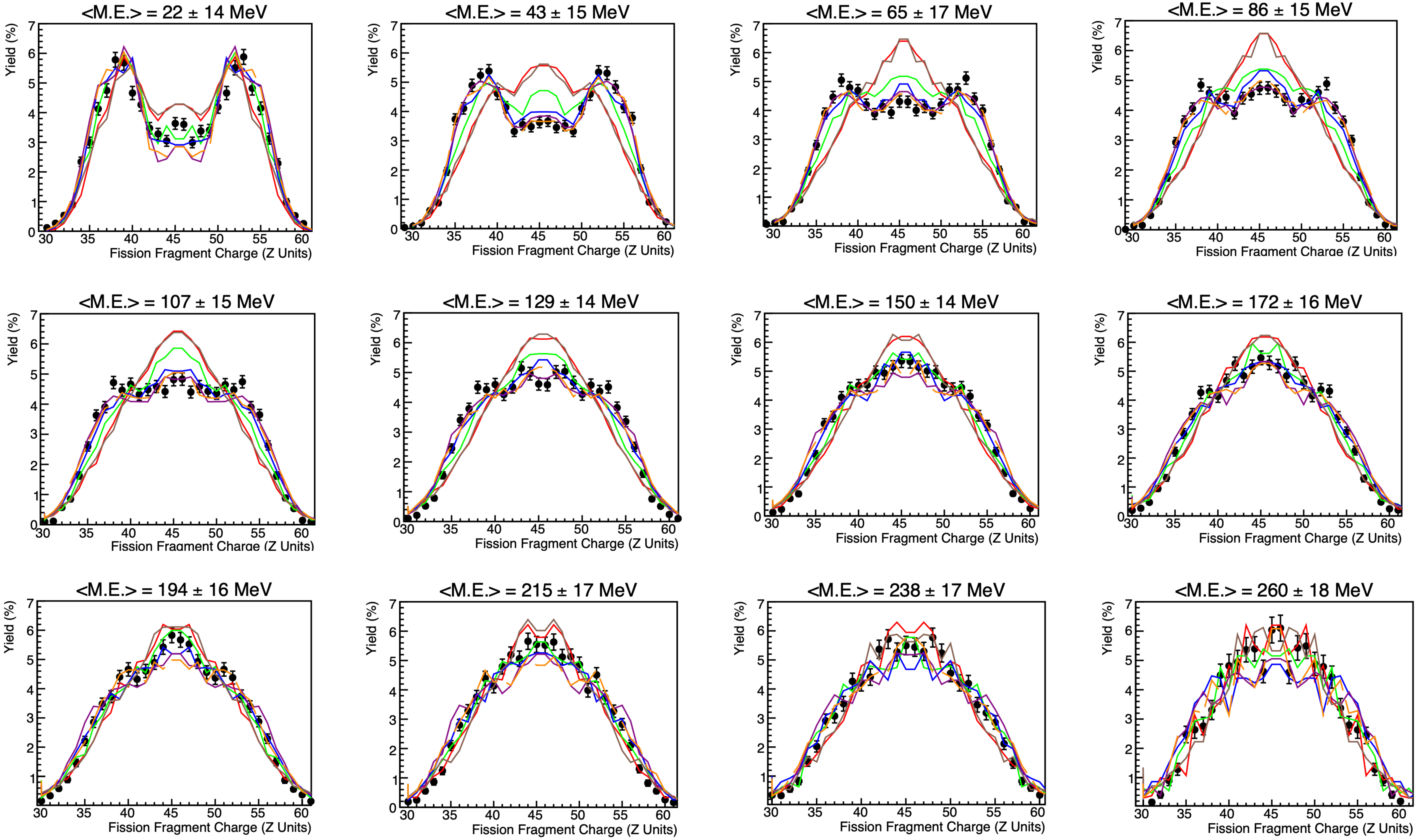

$$S(E^*) = \exp(-E^*/E_0)$$

- $E_0 = 10$ MeV
- $E_0 = 15$ MeV
- $E_0 = 20$ MeV
- $E_0 = 30$ MeV
- $E_0 = 40$ MeV

$$S(E^*) = \frac{1 + e^{-E_1/E_0}}{1 + e^{(E^* - E_1)/E_0}}$$

- $E_0 = 15,\ E_1 = 20$ MeV

Fission Fragment Evolution: Missing Energy

Theoretical opening angle distributions

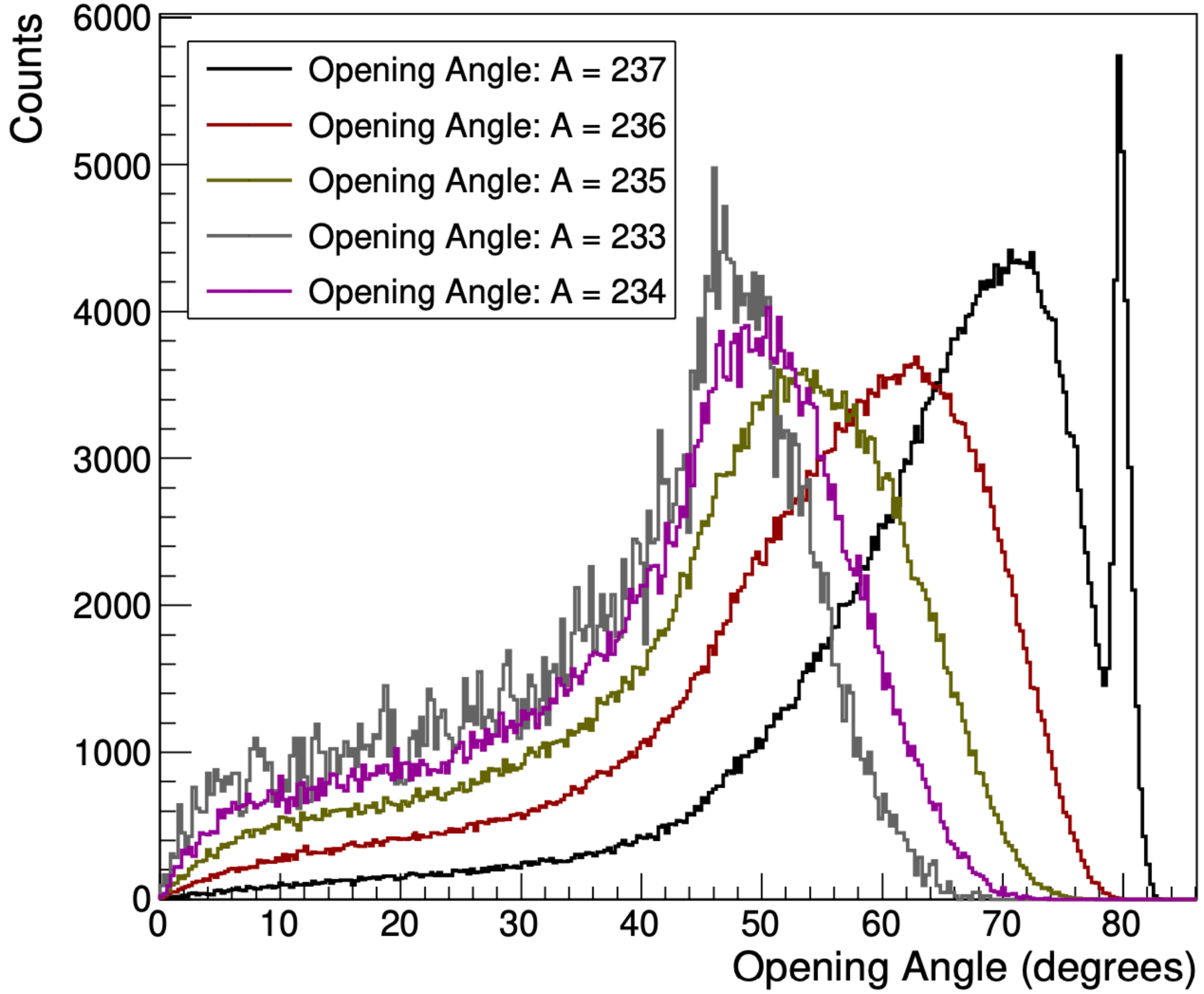

$$S(E^*) = \exp(-E^*/E_0)$$

$E_0 = 10$ MeV

$E_0 = 15$ MeV

$E_0 = 20$ MeV

$E_0 = 30$ MeV

$E_0 = 40$ MeV

$$S(E^*) = \frac{1 + e^{-E_1/E_0}}{1 + e^{(E^* - E_1)/E_0}}$$

$E_0 = 15,\ E_1 = 20$ MeV

Fission Fragment Evolution: Missing Energy

Theoretical opening angle distributions

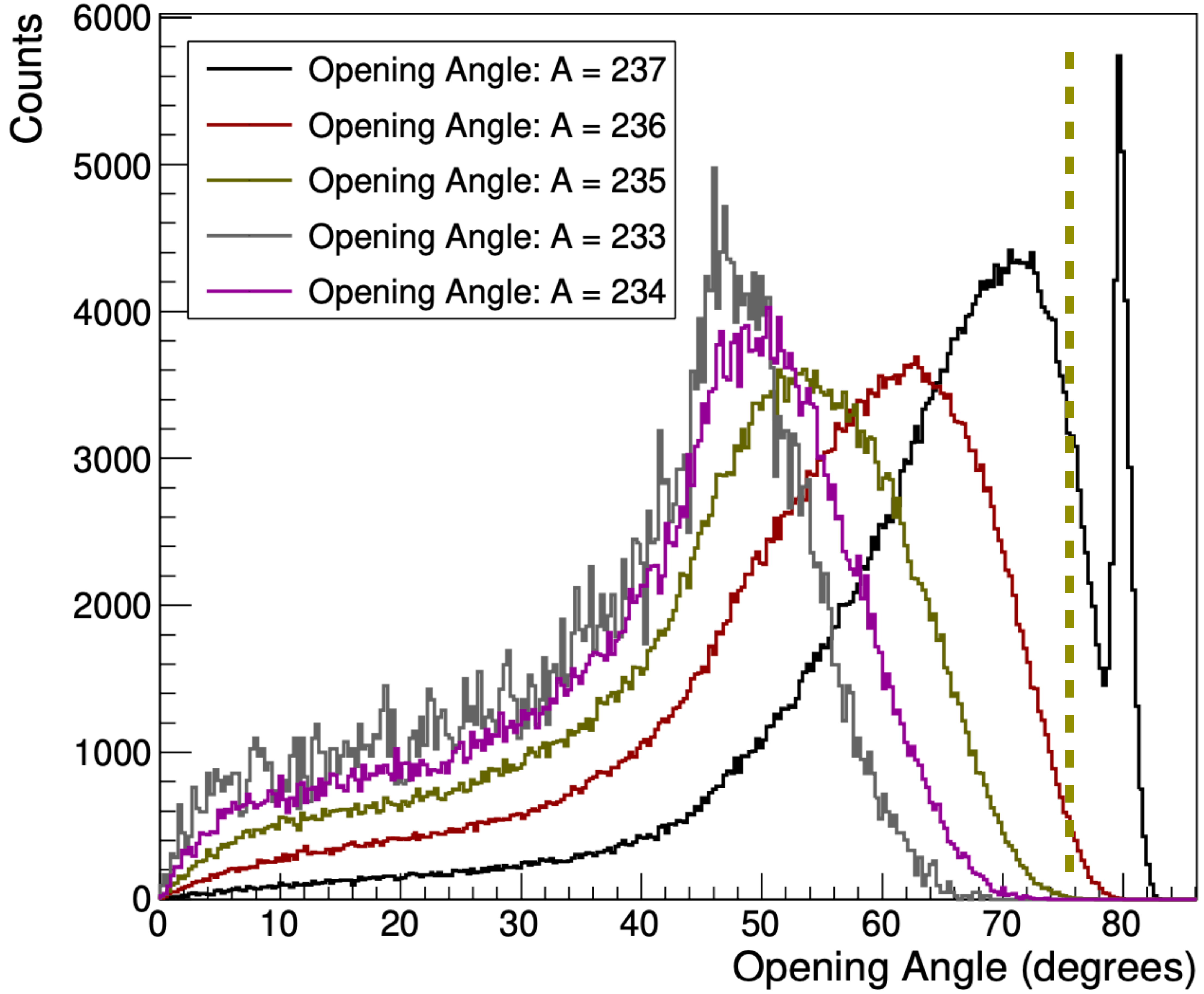

$$S(E^*) = \exp(-E^*/E_0)$$

- $E_0 = 10$ MeV
- $E_0 = 15$ MeV
- $E_0 = 20$ MeV
- $E_0 = 30$ MeV
- $E_0 = 40$ MeV

$$S(E^*) = \frac{1 + e^{-E_1/E_0}}{1 + e^{(E^* - E_1)/E_0}}$$

- $E_0 = 15,\ E_1 = 20$ MeV

Fission Fragment Evolution: Missing Energy

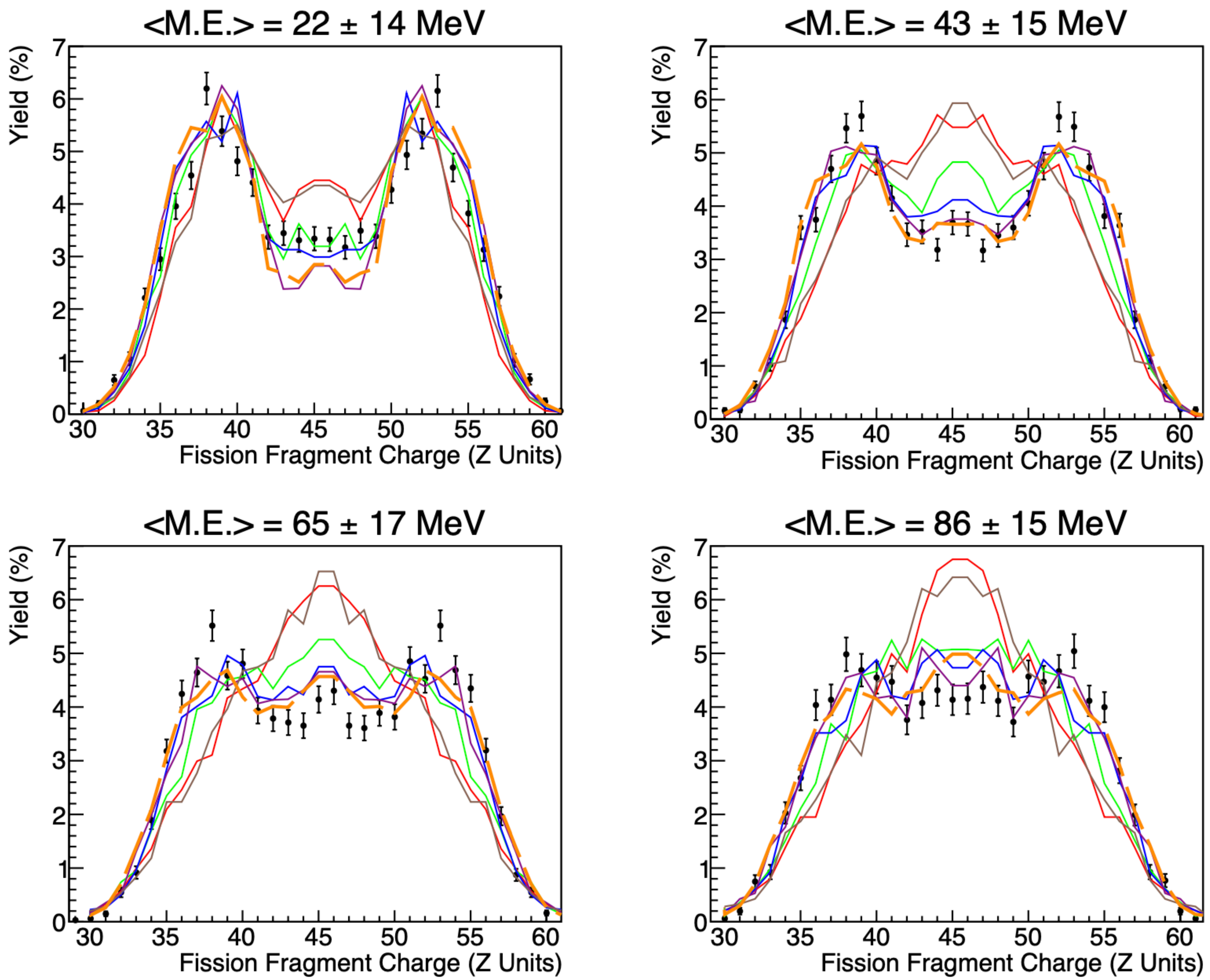

$S(E^*) = \exp(-E^*/E_0)$

- $E_0 = 10$ MeV
- $E_0 = 15$ MeV
- $E_0 = 20$ MeV
- $E_0 = 30$ MeV
- $E_0 = 40$ MeV

$$S(E^*) = \frac{1 + e^{-E_1/E_0}}{1 + e^{(E^* - E_1)/E_0}}$$

- $E_0 = 15,\ E_1 = 20$ MeV

Cross-Sections: Spallation-Fission Channels

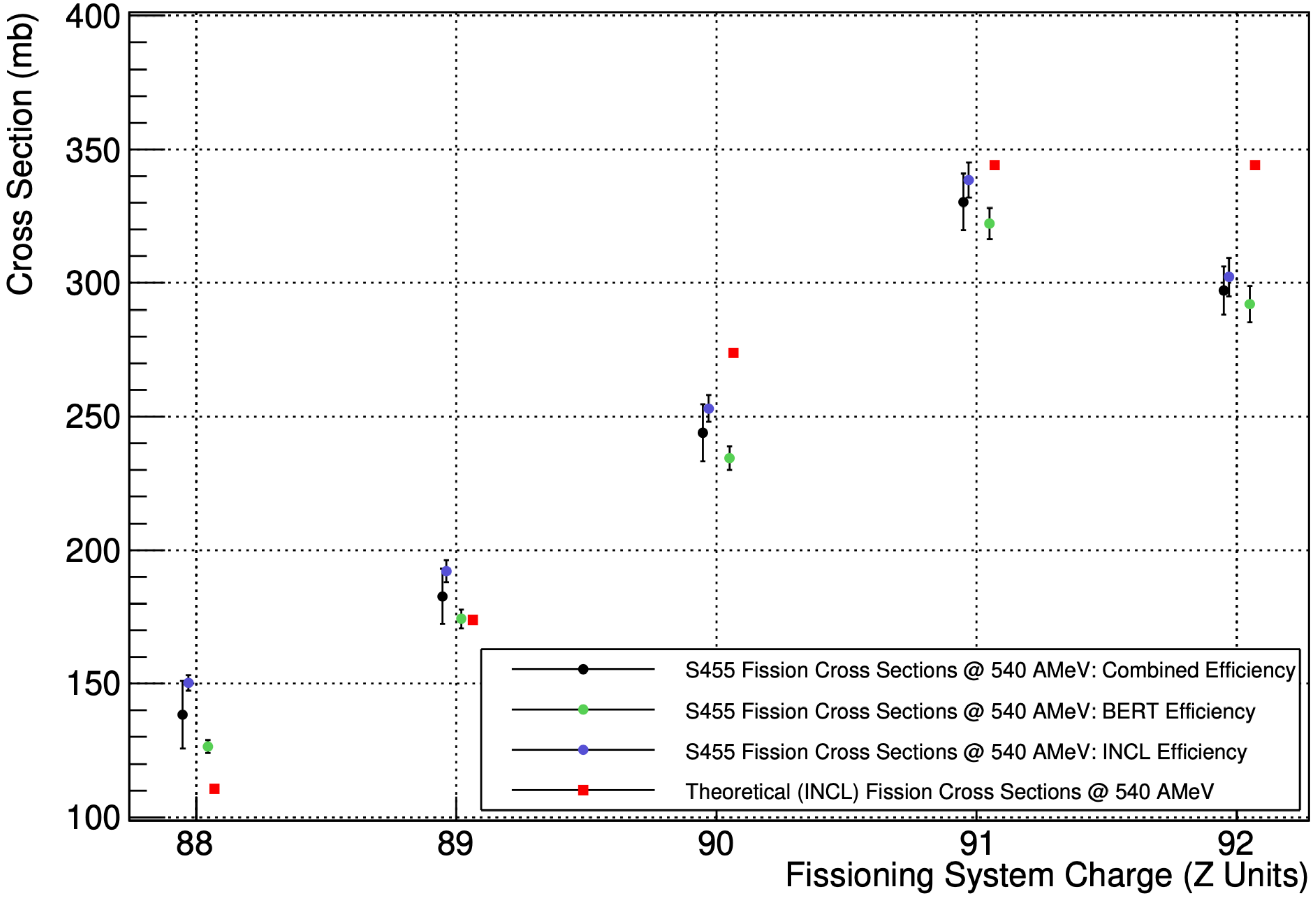

$Z_1 + Z_2$	σ_{INCL}	σ_{BERT}	$\sigma_{\mathrm{Combined}}$	σ_{Theory}
92	302 ± 7 mb	292 ± 7 mb	297 ± 9 mb	344 mb
91	338 ± 7 mb	322 ± 6 mb	330 ± 11 mb	344 mb
90	253 ± 5 mb	234 ± 4 mb	244 ± 11 mb	274 mb
89	192 ± 4 mb	173 ± 4 mb	183 ± 10 mb	173 mb
88	150 ± 3 mb	126 ± 2 mb	138 ± 13 mb	111 mb

$$\sigma = \frac{1}{2} \frac{N_r\ D\ M}{N_i\ \rho\ w\ N_A\ C_{\mathrm{OR}}\ \varepsilon_{Califa}\ (1 - dt)\ \varepsilon_{Twin}\ \varepsilon_{TPat}}$$

Cross-Sections: Spallation-Fission Channels

$Z_1 + Z_2$ (Quasi-free)	σ_{INCL}	σ_{BERT}	σ_{Combined}	σ_{Theory}
91	3.12 ± 0.07 mb	2.89 ± 0.05 mb	3.03 ± 0.12 mb	3.18 mb

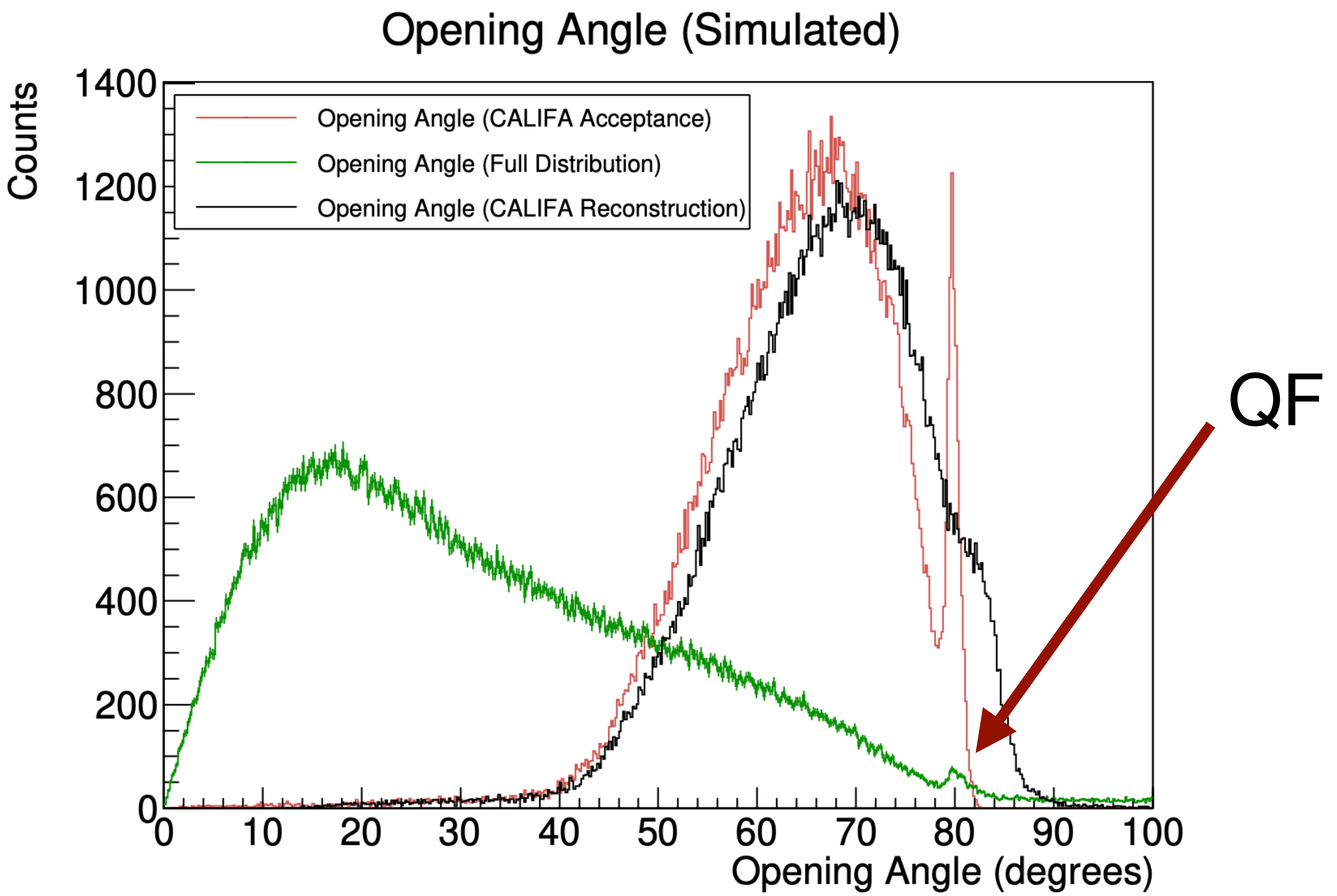

Cross-Sections: Spallation-Evaporation Channels

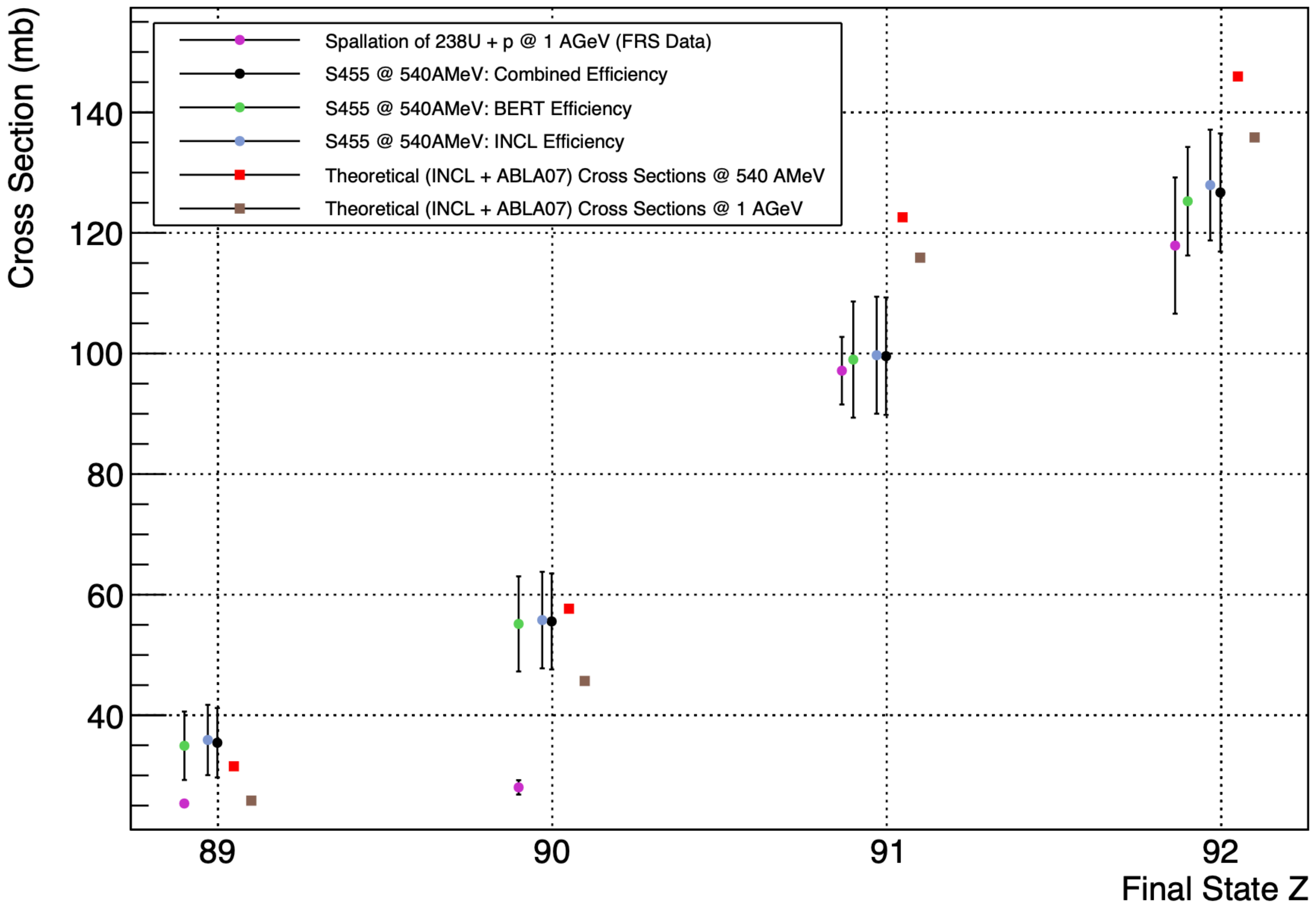

$$\sigma = \frac{1}{2}\frac{F\, N_r\, D\, M}{N_i\, \rho\, w\, N_A\, C_{OR}\, \varepsilon_{Califa}\, (1-dt)\, \varepsilon_{Twim}\, \varepsilon_{TPat}}$$

Cross-Sections: Spallation-Evaporation Channels

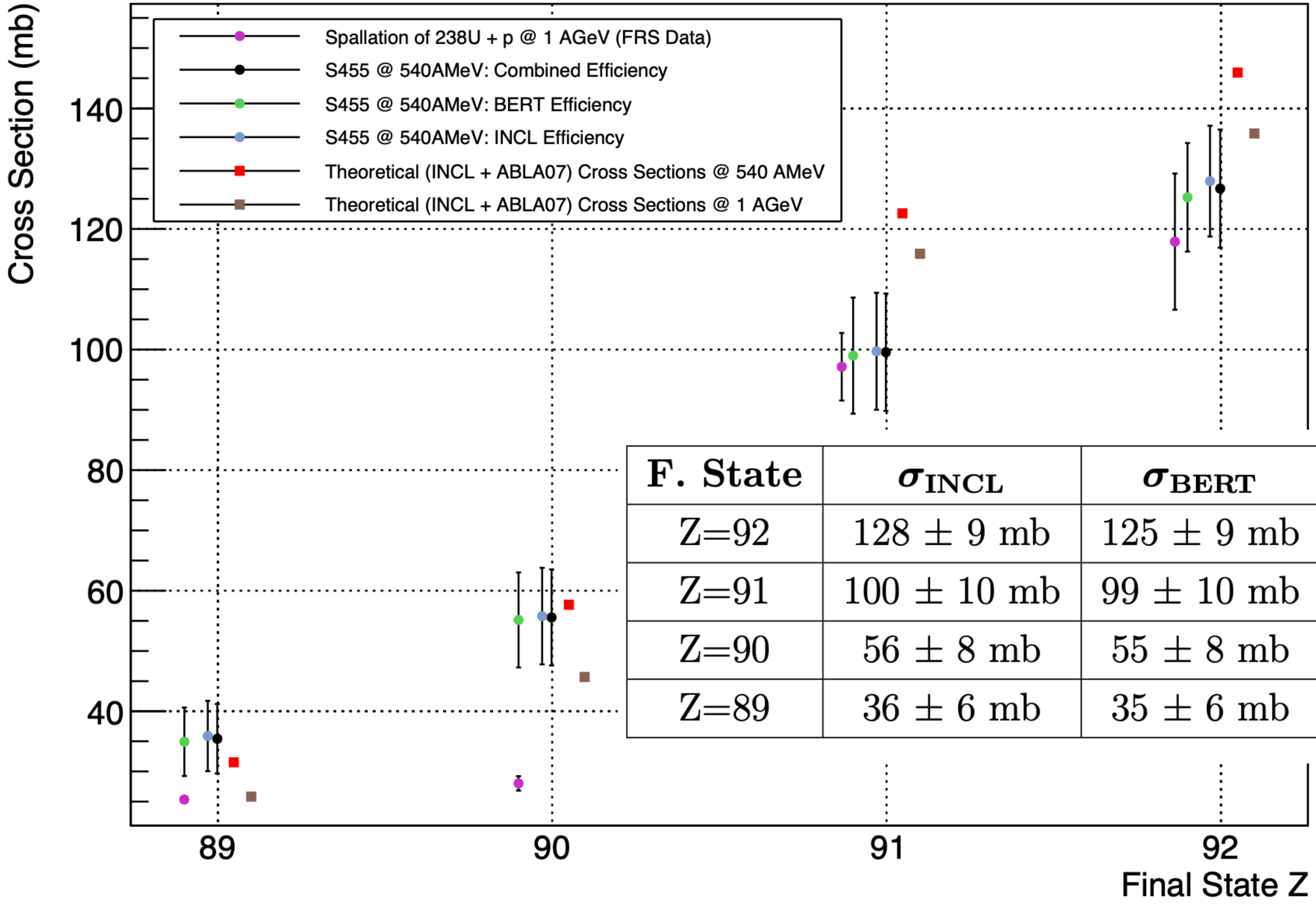

$$\sigma = \frac{1}{2} \frac{F\, N_r\, D\, M}{N_i\, \rho\, w\, N_A\, C_{OR}\, \varepsilon_{Califa}\, (1-dt)\, \varepsilon_{Twim}\, \varepsilon_{TPat}}$$

F. State	σ_{INCL}	σ_{BERT}	$\sigma_{Combined}$	σ_{Theory}	σ([82])	σ_{Theory}([82])
Z=92	128 ± 9 mb	125 ± 9 mb	126 ± 10 mb	146 mb	118 ± 11 mb	136 mb
Z=91	100 ± 10 mb	99 ± 10 mb	99 ± 10 mb	122 mb	97 ± 6 mb	116 mb
Z=90	56 ± 8 mb	55 ± 8 mb	55 ± 8 mb	57 mb	28 ± 1 mb	45 mb
Z=89	36 ± 6 mb	35 ± 6 mb	35 ± 6 mb	31 mb	25 ± 1 mb	26 mb

[82]: *J. Taieb et al. Evaporation residues produced in the spallation reaction $^{238}U + p$ at 1 AGeV. Nuclear Physics A, 724, 2003.*

Cross-Sections: Spallation-Evaporation Channels

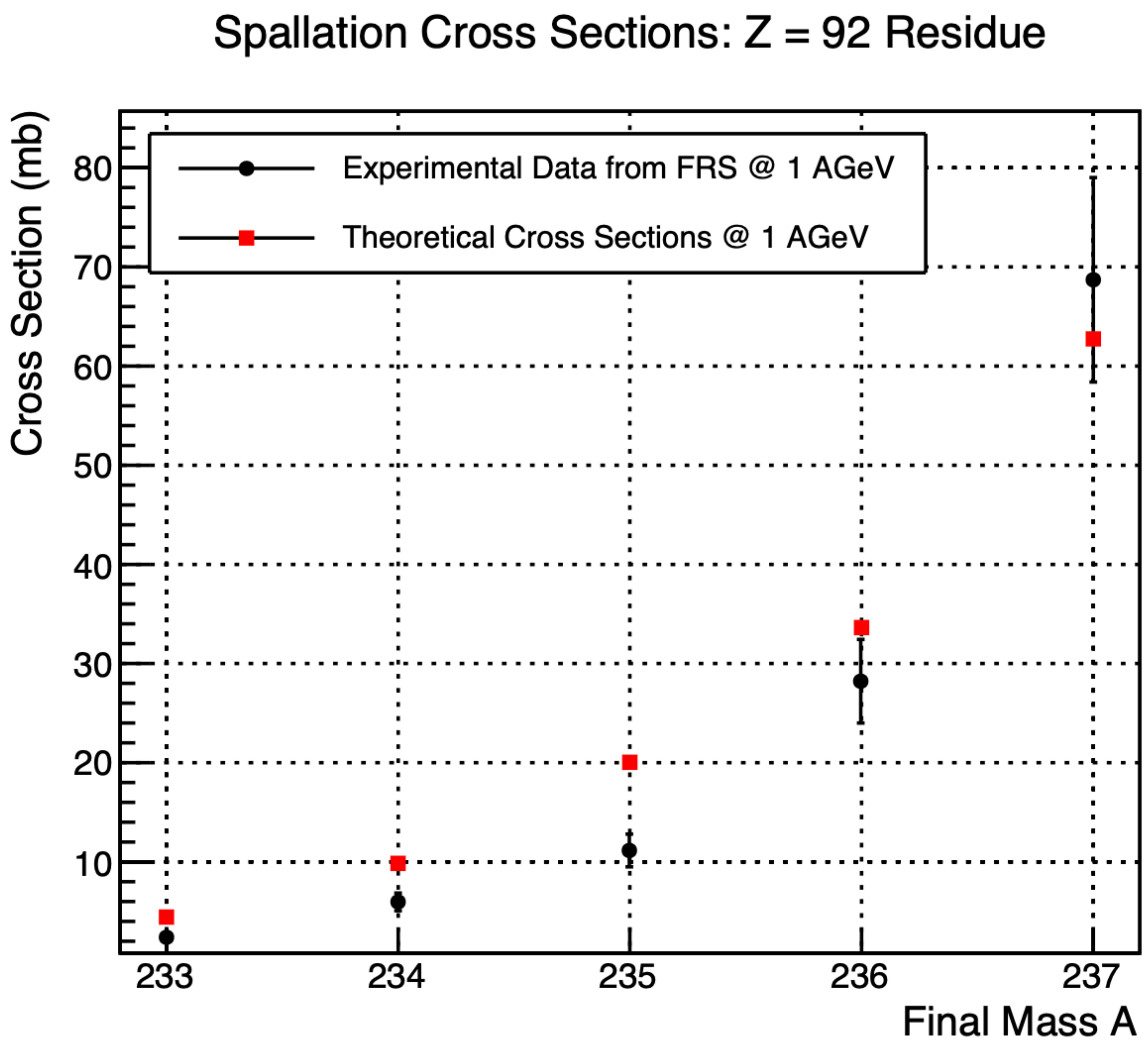

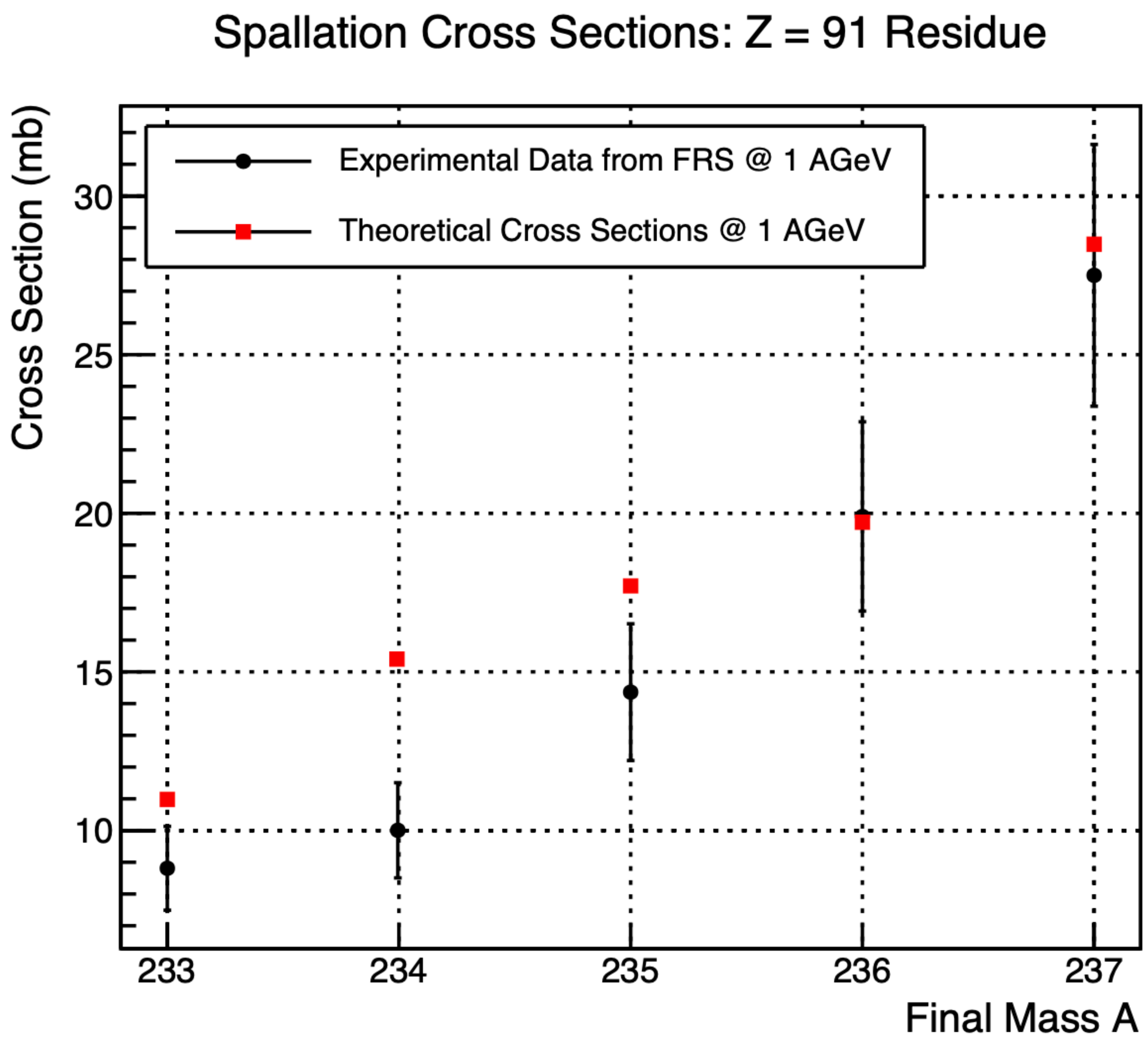

Conclusions

1. **First** experiment on **knockout-induced fission** of ^{238}U has been carried out at GSI to study the evolution of the fission fragments with the excitation energy.

2. A NN **algorithm** was developed for CALIFA punch-through reconstruction. **Resolutions** around **7-10%** were obtained, which are better than previous studies with test crystals.

3. The obtained kinematical and angular distributions, and the reconstructed fission fragment charges allowed for insightful correlations between these observables.

4. The reconstructed **missing energy** correlated with the observed **fission fragment charge yields** allowed for the test of theoretical models. It was found that an **exponential** damping functions with a constant parameter of 40 MeV and the parameterization from **Randrup** and **Möller**, with values of $E_0 = 15$ and $E_1 = 20$ MeV, are the prescriptions that better describes the experimental yields.

Conclusions

5. Theoretical and experimental values for **fission cross-sections** are in **good agreement**. The calculated cross-section of 330 $\pm$ 11 mb for Protactinium fission allowed for an estimation of the **quasi-free mechanism**, with a final value of 3.03 ± 0.12 mb.

6. **Spallation cross-sections** were also obtained and compared with theory and previously measured experimental data at FRS. The largest disagreement (~ 20 %) was found for both $Z = 92$ and $Z = 91$ final systems, for this **experiment** and for previous ones at **FRS**.


Thank You !

Backup Slides

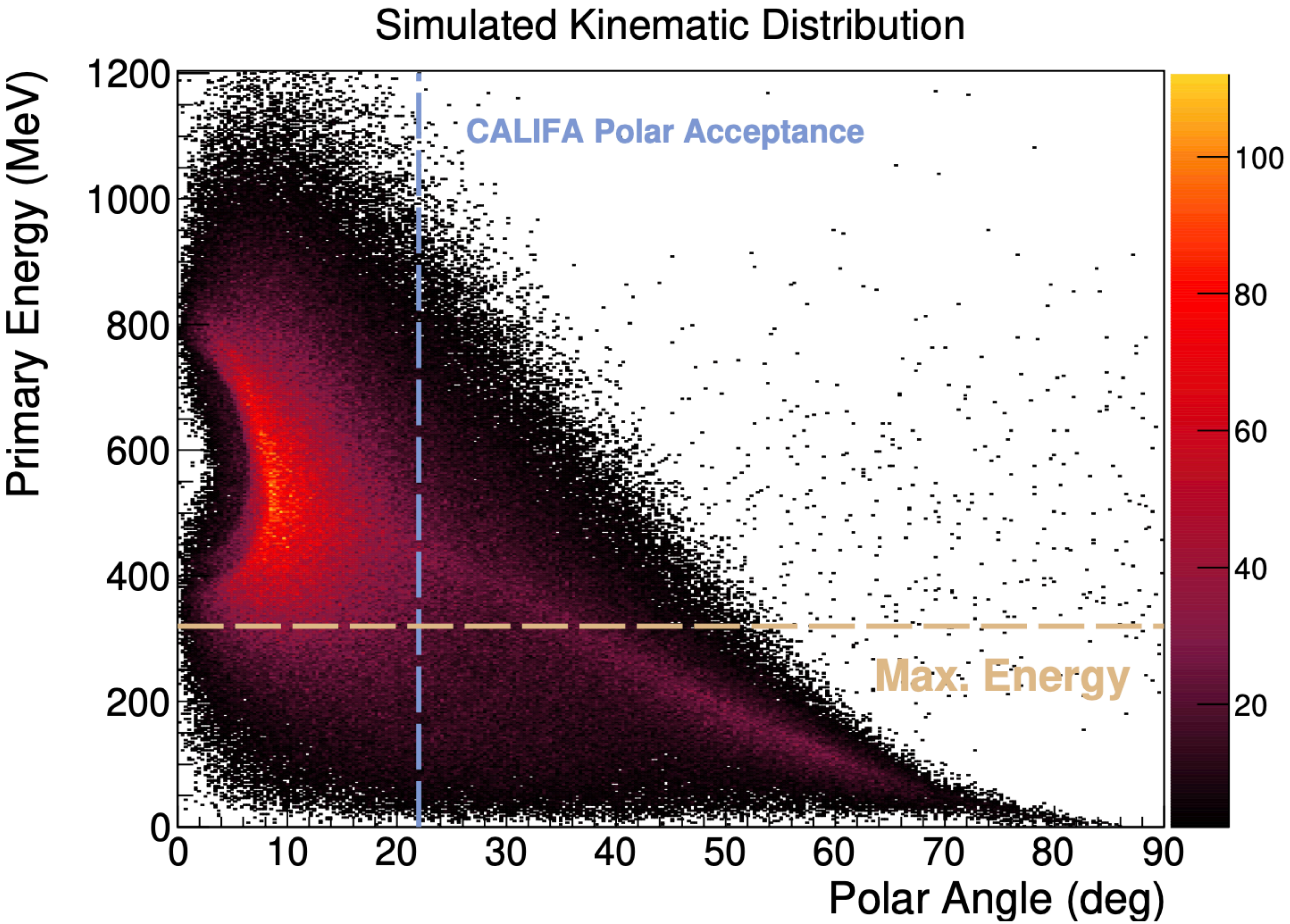

Simulated Kinematic Distribution
Primary Energy (MeV)
Polar Angle (deg)
CALIFA Polar Acceptance
Max. Energy
0
200
400
600
800
1000
1200
0
10
20
30
40
50
60
70
80
90
20
40
60
80
100

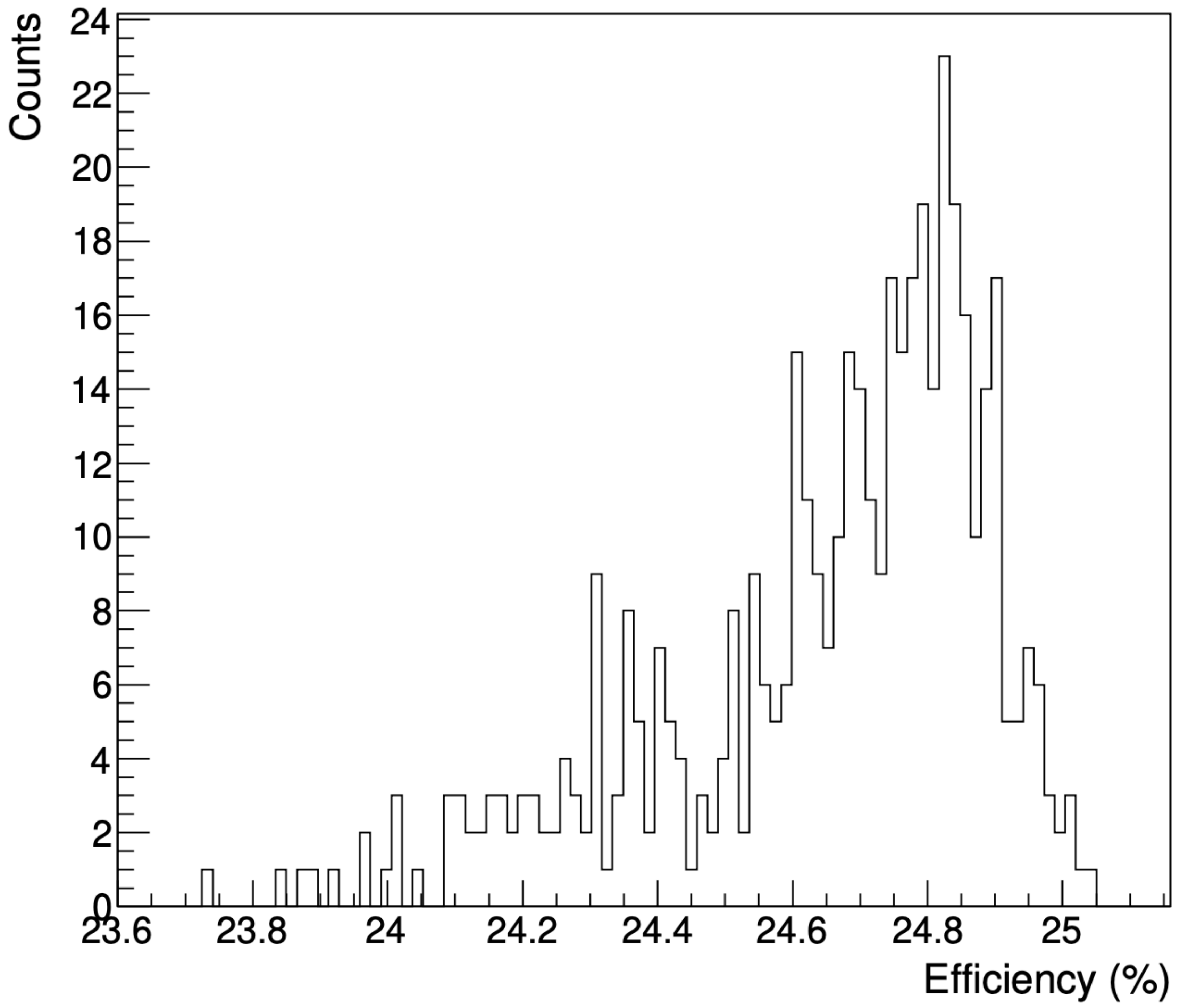
Counts
24
22
20
18
16
14
12
10
8
6
4
2
0
23.6
23.8
24
24.2
24.4
24.6
24.8
25
Efficiency (%)

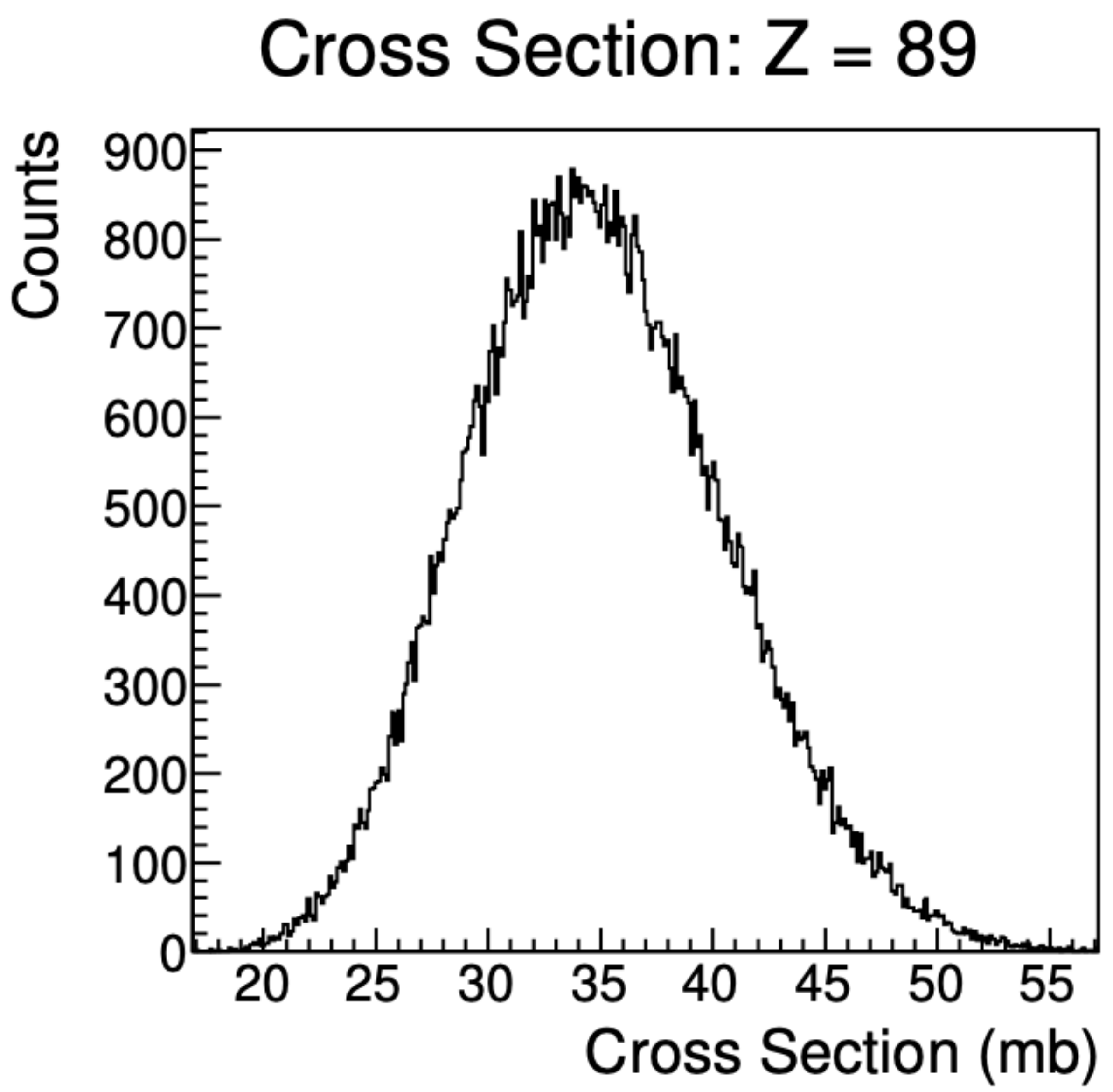
Cross Section: Z = 89
Counts
900
800
700
600
500
400
300
200
100
0
20
25
30
35
40
45
50
55
Cross Section (mb)

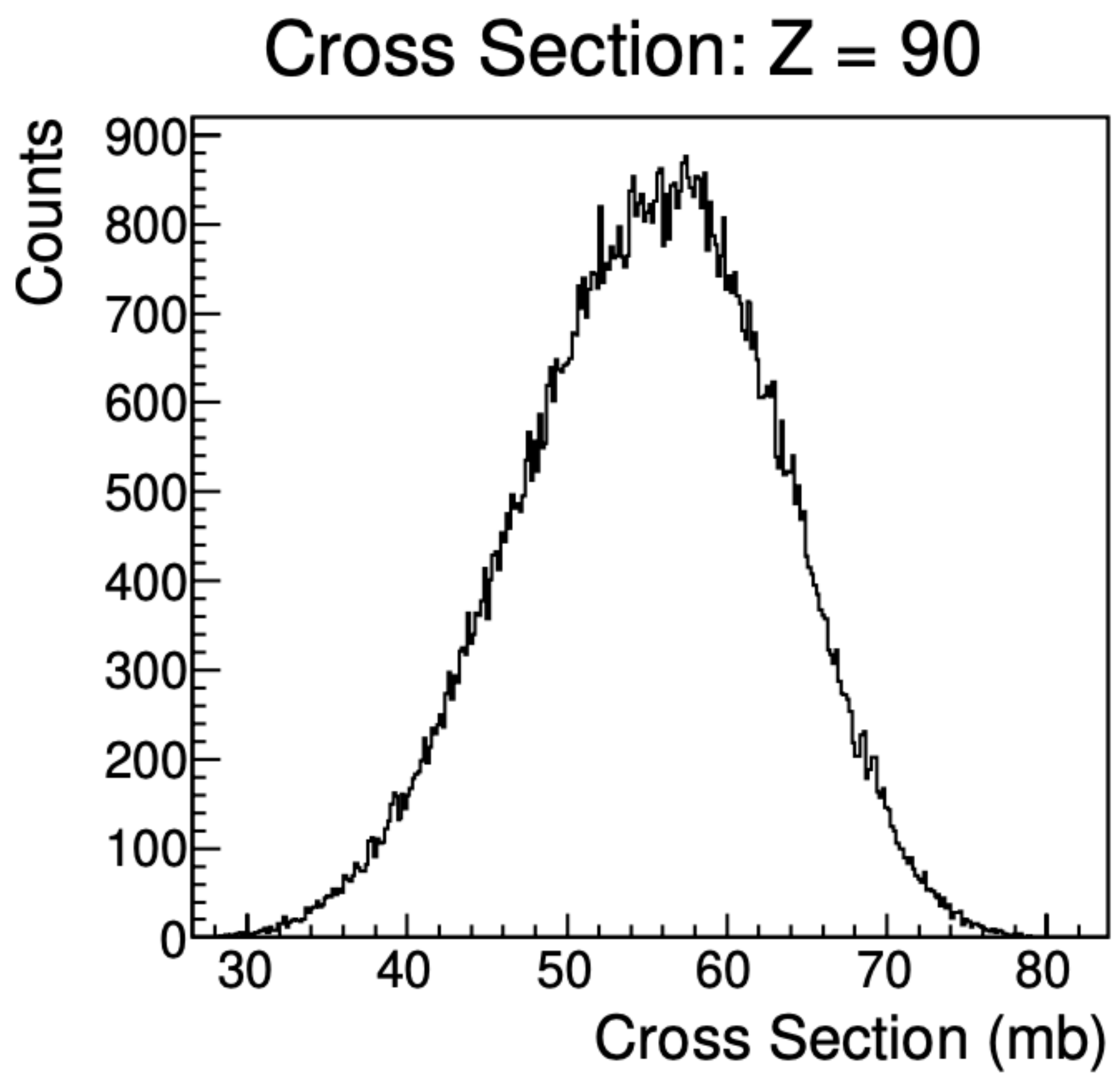
Cross Section: Z = 90
Counts
900
800
700
600
500
400
300
200
100
0
30
40
50
60
70
80
Cross Section (mb)

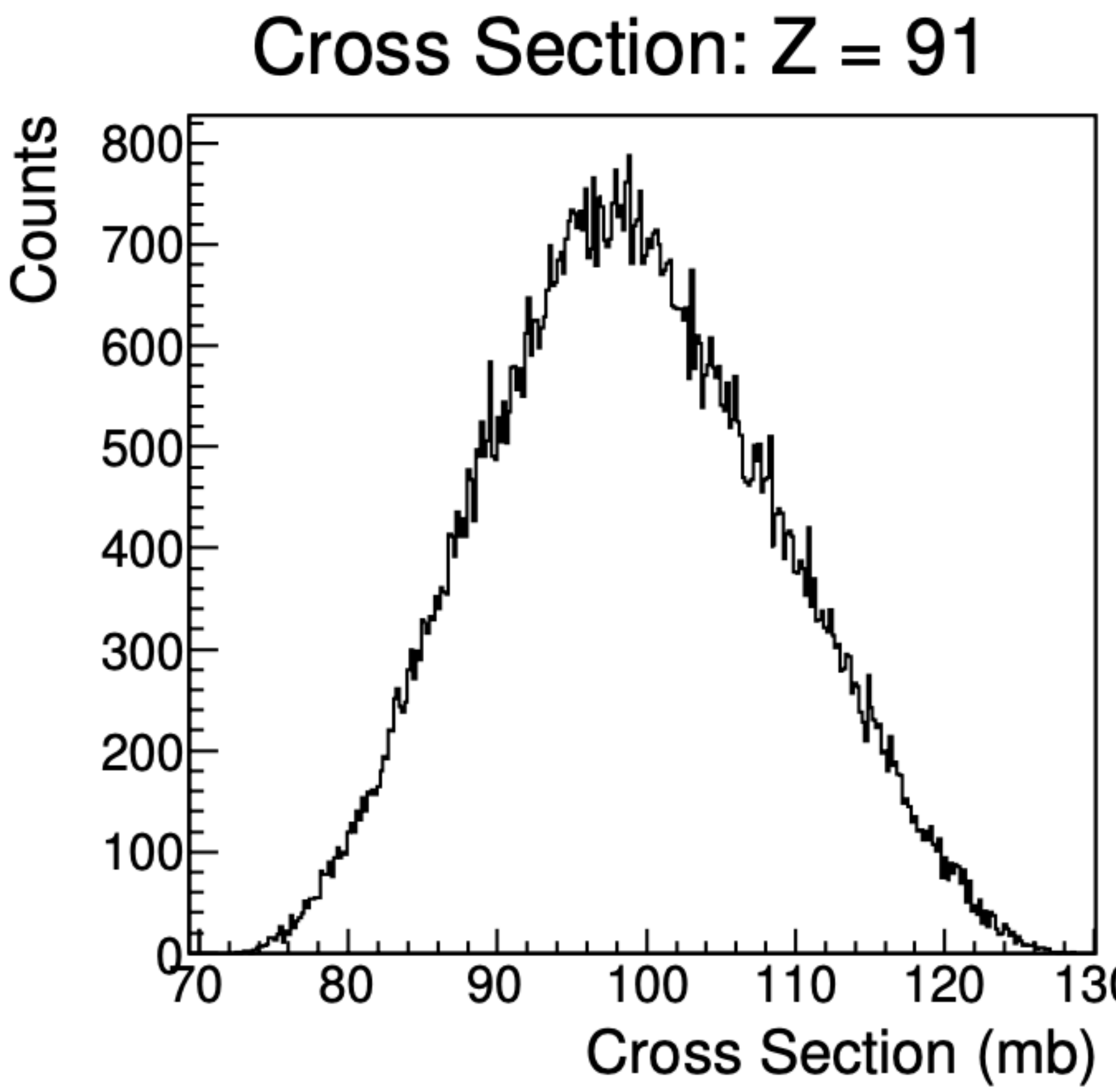
Cross Section: Z = 91
Counts
800
700
600
500
400
300
200
100
0
70
80
90
100
110
120
130
Cross Section (mb)

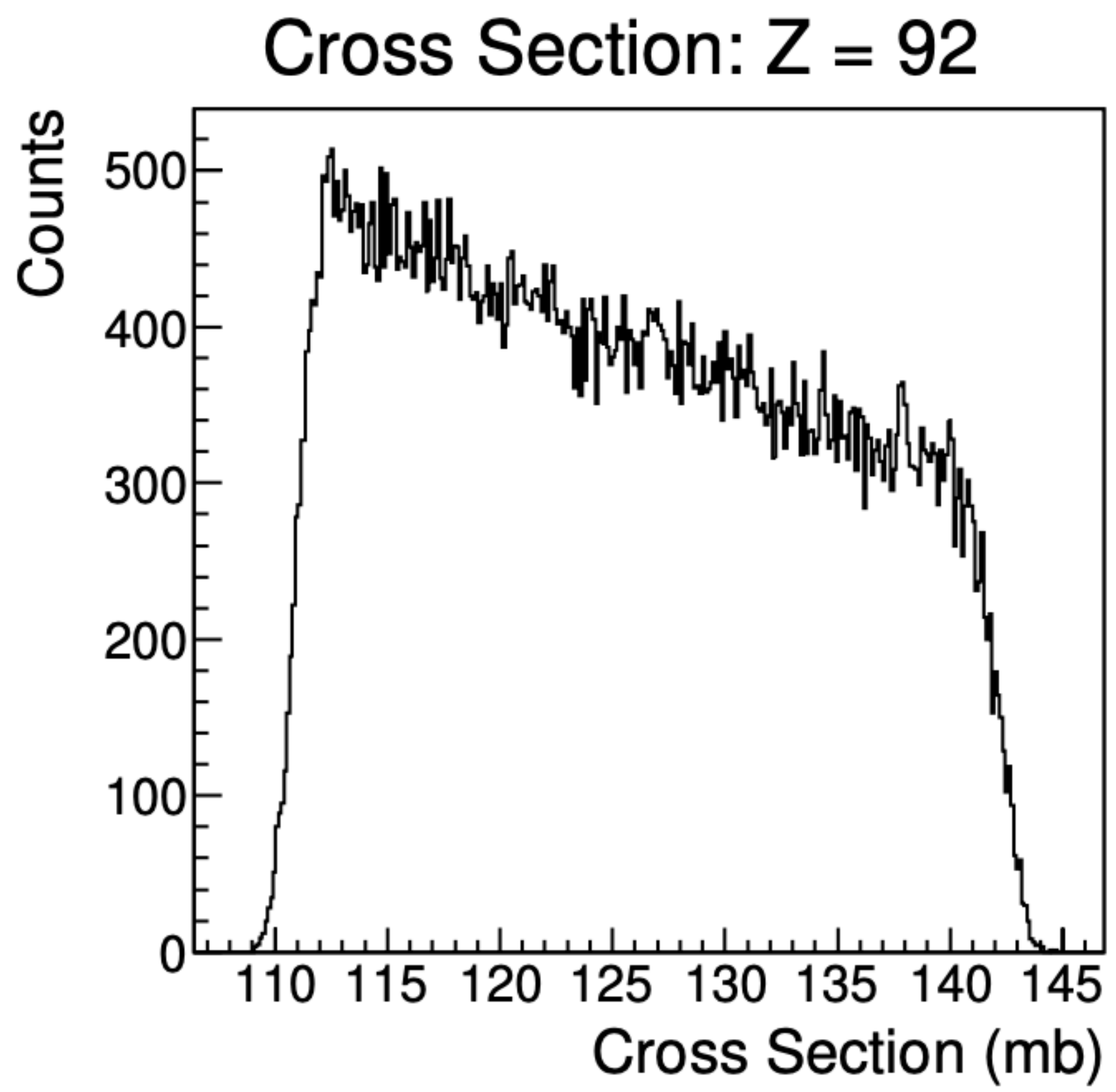
Cross Section: Z = 92
Counts
500
400
300
200
100
0
110
115
120
125
130
135
140
145
Cross Section (mb)

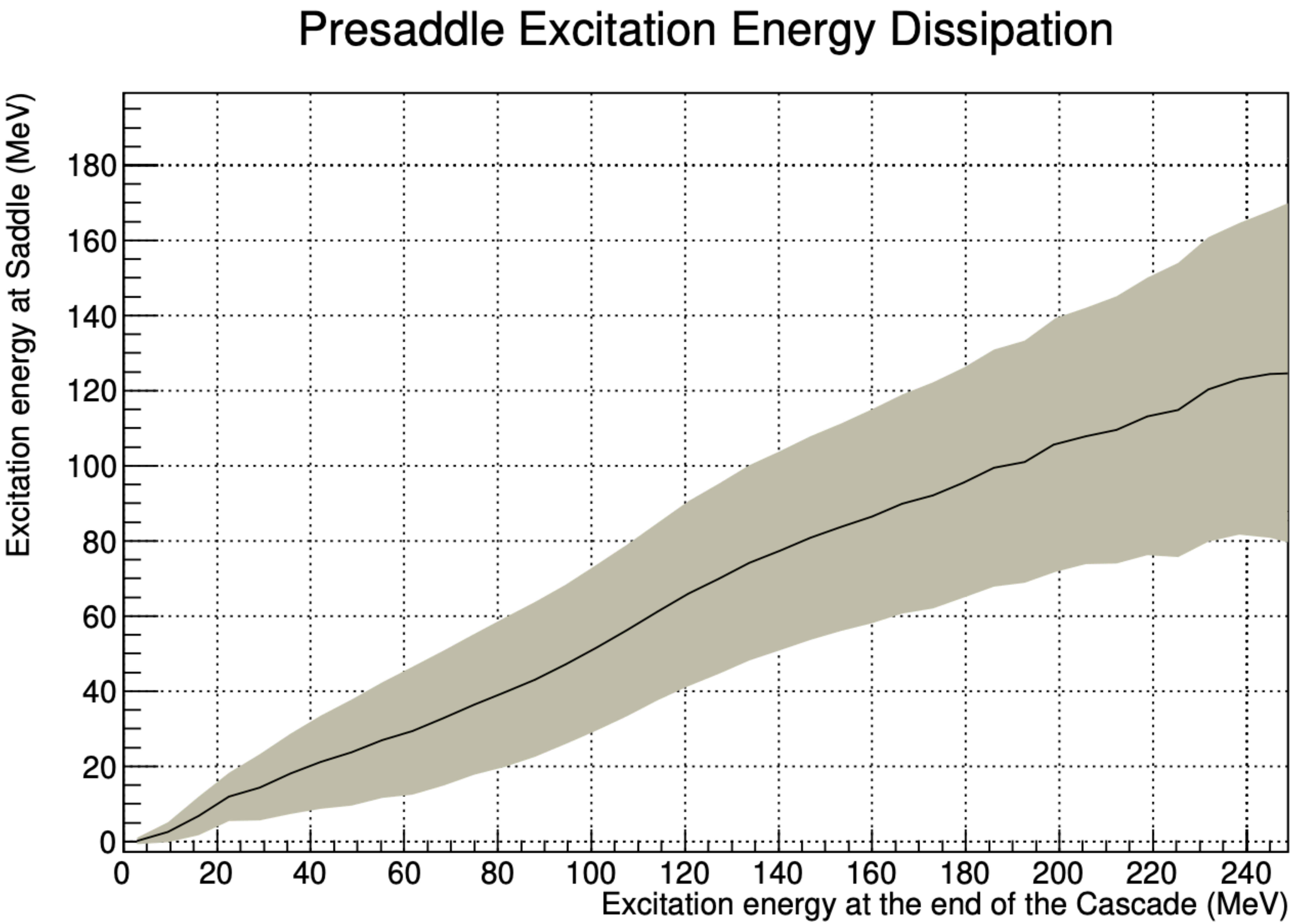
Presaddle Excitation Energy Dissipation
Excitation energy at Saddle (MeV)
0
20
40
60
80
100
120
140
160
180
0
20
40
60
80
100
120
140
160
180
200
220
240
Excitation energy at the end of the Cascade (MeV)